ISSN NO. 2320-5407

Journal homepage: http://www.journalijar.com

INTERNATIONAL JOURNAL OF ADVANCED RESEARCH

RESEARCH ARTICLE

Synthesis and Characterization of Copper(II) Complexes Containing Sulfur/Nitrogen Donor Sets. Mimicking the Function of Phenoxazinone Synthase and Catechol Oxidase

Abd El-Motaleb M. Ramadan[1*], Youssef L. Aly[1], Saied M. E. Khalil[2], Magdy Shebl[2] and Ramy A. S. El-Naem[1]

1.Chemistry Department, Faculty of Science, Kafr El-Sheikh University, Kafr El-Sheikh Egypt
2.Chemistry Department, Faculty of Education, Ain Shams University, Roxy, Cairo, Egypt

Manuscript Info

Manuscript History:

Received: 15 May 2015
Final Accepted: 22 June 2015
Published Online: July 2015

Key words:

Sulfur/Nitrogen donor sets, copper(II) complexes, biomimetic catalytic activity, catechol oxidase, phenoxazinone synthase, Kinetic measurements, functional models.

Corresponding Author

Abd El-Motaleb M. Ramadan

Abstract

Copper(II) complexes of the pentadentate pyridine based ligand (L^1) containing two thiolate sulfur, pyridine nitrogen and two azomethines nitrogen, in addition to a series of tetradentate ligands (L^2, L^3 and L^4) containing two thiolate sulfur, and two azomethine nitrogens have been synthesized (scheme 1). The pure isolated complexes have been characterized by elemental analyses; electrolytic conductance, magnetic susceptibility measurements, FT-IR, UV–Vis and ESR spectroscopy and their structures have been confirmed by thermal analysis (TGA and DTG) investigations. All these green colored copper(II) complexes are hydrated containing one coordinated water molecule. The solid and solution states investigations show that the complexes are neutral. The pyridine based Schiff base (L^1) acts as dibasic N_3S_2 chelating ligand coordinating to Cu(II) center and the coordination geometry around copper(II) center of $[CuL^1H_2O]$ (**1)** is a distorted octahedron. The five coordinated copper(II) complexes $[CuL^nH_2O]$ of the dibasic tetradentate ligands L^2, L^3 and L^3 having the coordination chromophore N_2S_2O exhibit structural features similarity. The coordination geometries around copper(II) centers in (**2)**, (**3)** and (**4)** are described as square pyramidal stereochemistry based upon the EPR and crystal filed spectral results. The electrochemical properties behaviors of the chelates have been studied by cyclic voltammetry technique. Mimicking the function of phenoxazinone synthase and catechol oxidase enzymes investigations demonstrated that, the title complexes are promising functional models of these oxidase metalloproteins containing copper. Oxidative coupling of 2-aminophenol (OAPH) to 2-aminophenoxazine-3-one (APX) (phenoxazinone synthase activity) and the aerobic oxidation of 3,5-di-tert-butylcatechol (3,5-DTBCH_2) to the light absorbing 3,5-di-tert-butyl-benzoquinone (3,5-DTBQ) (catechol oxidase activity), catalyzed by the title copper(II) complexes were studied. The rate constants of the above oxidation reactions showed linear dependence on catalyst concentration and saturation kinetics with respect to the corresponding substrate. Electrochemical data revealed a non-linear relationship between the complexes ability to oxidize the studied substrates (OAPH and 3,5-DTBCH_2) and their redox potentials. Also, the present catalytic investigations demonstrated that the geometrical effects are only one facet of the complexes activity. Addition of Lewis base, triethylamine, in both systems exhibits dramatic effect on the rate of these catalytic aerobic oxidation reactions. The probable mechanistic implications of both catalytic systems are discussed.

INTRODUCTION

The potential role played by copper ions in the active sites of a large number of metalloprotein has stimulated efforts to design and characterize copper complexes as models for providing better understanding of biological systems and for assisting in the development of new homogeneous catalysts for selective oxidation. Particularly, the coordination chemistry and reactivity of copper complexes involving nitrogen–sulfur donor ligands has received considerable attention as models (Holm et al., 2004; Harrop et al., 2004; Lobana et al., 2004; Selman et al.; 2004; Reddy et al., 2004; Dhar et al., 2003, Santra et al., 2001). In particular the CuN_2S_2 chromophore is present in blue copper proteins such as plastocyanin (Holm et al., 1996; Ali et al., 1987) and copper(II) chelates of SNNS ligands have been found to have antineoplastic activities and to interact with biological systems (Minkel et al., 1978; 1976; 1976).

Nowadays, efforts have been devoted to the design and synthesis of structurally flexible N/S donor ligands that can adopt various coordination modes (Ronson et al., 2006; Tavacoli et al., 2003). The main objective is to produce new functional materials with specific molecular arrangements capable of showing the desirable properties (Argent et al., 2006; Xie et al., 2005). With flexible ligands, the competition between chelating and bridging coordination modes is an important factor in producing mono, di, and polynuclear metal complexes (Gennari et al., 2007; Wang et al., 2007; Ganesamoorthy et al., 2007; Liaw et al., 2007).

The synthesis and reactivity studies of transition metal complexes as structural and functional models for metalloenzymes with oxidase activity are of particular interest for the development of bioinspired catalysts for oxidation reactions. The oxidative coupling of 2-aminophenol (OAPH) to 2-aminophenoxazine-3-one (APX) through catalytic activation of dioxygen by transition metal complexes has been considered as one of the important reactions because of the presence of 2-aminophenoxazine chromophore (APX) in Actinomycin D a naturally occurring antibiotic. The enzyme phenoxazinone synthase, a type 2 copper-containing oxidase (subunit molecular mass 88 000, 3.7 Cu per subunit) (Barry et al., 1989) is naturally found in the bacterium Streptomyces antibiotics and has been cloned and over expressed in S. lividians (Jones et al., 1984). It catalyzes the oxidative coupling of two molecules of a substituted 2-aminophenol (OAPH) to the phenoxazinone chromophore (APX) in the final step of the biosynthesis of actinomycin D (Barry et al., 1988). The reaction represents a six-electron oxidative coupling and appears to take place stoichiometrically in a series of three two-electron oxidation steps. Cyclization occurs with the concomitant reduction of molecular oxygen to water. Actinomycin D is among the most potent antineoplastic agents known. It inhibits DNA directed RNA synthesis (Homma et al., 1962) and is used clinically in the treatment of some kind of cancer of the bones and soft tissues like Choriocarcinoma, testis, Wilm's tumor, rhabdomyosarcoma, Kaposi's sarcoma and Ewing's sarcoma due to their higher toxicity (Katz et al., 1962). Many works were dedicated in the past years for considerable numbers of functional models based on manganese, cobalt, iron and copper have been reported which mimic the catalytic activity of phenoxazinone synthase (Prati et al., 1992, Horvath et al., 2004, Szeverenyi et al., 1991, Simandi et al., 1993, 1996, 2004, 2003, Maurya et al., 2005, El-Khalafy et al., 2012, Hassanein et al., 2008, Mukherjee et al., 2007, Bakshi et al., 2012, Panja 2012, Olmazu et al., 2012)

Catechol oxidase is another copper enzyme, isolated from phytogenic materials, only catalyses the oxidation of catechol to quinone without acting on tyrosinase. This reaction is of great importance in medical diagnosis for the determination of the hormonally active catecholamine adrenaline, noradrenalin and dopamine (Than et al., 1999). Secondary reactions (melanin formation) follow the oxidation of the substrate in presence of polyphenol oxidase, which causes the brown color of the injured plants. Functional models of catechol oxidase have been extensively studied using copper (Gentschev et al., 2000, Ramadan et al., 2006, 2011, 2012) iron (May et al., 2006; Simandi et al., 2005; Ramadan et al., 1998) cobalt (Simandi et al., 2003) manganese (Szigyarto et al., 2006; Blay et al., 2006; Majumder et al., 2006; Ramadan et al., 1998) and recently vanadium (Ramadan et al., 2012) complexes as catalysts. However, the mechanism of these oxidase native enzymes (catechol oxidase and phenoxazinone synthase) and the functional model metal complexes still also remains far from clear. In addition to former only a limited number of catechol oxidase model systems in connection with the phenoxazinone synthase have been reported (Kaizer et al., 2008; 2005; Horvath et al., 2004).

In continuation of our earlier work in the area of copper(II) chemistry we describe here in this contribution the synthesis and characterization of a series of copper(II) complexes containing sulfur and nitrogen donors as potential structural and functional models for the active sites of both catechol oxidase and phenoxazinone synthase. The oxidase biomimetic catalytic activity of these mononuclear copper(II) complexes have been measured in order to get insight about the structure and reactivity relation ship in addition to propose a plausible mechanism for these biomimetic reactions.

2. Experimental

2.1. Materials

All chemicals used were of analytical grade. The α- dicarbonyls used namely 2,3-dicarbonylbutane, 4,4-dimethoxybenzile and 2,3-dicarbonylpropane were purchased from Aldrich. 2,6-pyridinedicarbaldehyde was synthesized according to the method described elsewhere (Alcock et al., 1937) and 4-amino-6-methyl-5-oxo-3-(2H)-thioxo-1,2,4-triazine was prepared as reported in the literature.(Dornow et al., 1964).

2.2. Synthesis of copper(II) complexes **1**-**4**

The template condensation reaction of the reported dicarbonyl and 4-amino-6-methyl-5-oxo-3-(2H)-thioxo-1,2,4-triazine under the influence of the metal ions requires that the condensation be initiated before 4-amino-6-methyl-5-oxo-3-(2H)-thioxo-1,2,4-triazine is added. For this purpose an equimolar amounts (0.024 mol) of the reported dicarbonyl and $CuCl_2$ were mixed in 50 ml absolute ethanol and the reaction mixture was stirred for one hours at room temperature. While this reaction mixture solution was under stirring, a solution of 4-amino-6-methyl-5-oxo-3-(2H)-thioxo-1,2,4-triazine in 50 ml of absolute ethanol was added. The reaction mixture was further stirred at room temperature for 2 hours, during which time green products precipitated. After that, the solution of the reaction mixture was filtered and the isolated solid was washed with ethanol and ether and finally dried in vacuum over CaO at room temperature for two weeks.

2.3. Physical measurements

IR spectra were recorded using KBr disks in the 4000-200 cm^{-1} range on a Unicam SP200 spectrophotometer. The electronic absorption spectra were obtained in DMF solution with a Shimadzu UV-240 spectrophotometer. Magnetic moments were measured by Gouy's method at room temperature. ESR measurements of the polycrystalline samples at room temperature were made on a Varian E9 X-band spectrometer using a quartz Dewar vessel. All spectra were calibrated with DPPH (g = 2.0027). The specific conductance of the complexes was measured using freshly prepared 10^{-3} M solutions in electrochemically pure DMF at room temperature, using an YSI Model 32 conductance meter. The thermogravimetric measurements were performed using a Shimadzu TG 50-Thermogravimetric analyzer in the 25-800 °C range and under an N_2 atmosphere. Elemental analyses (C, H, and N) were carried out at the Micro analytical Unit of Cairo University.

2.4. Electrochemical measurements

Cyclic voltammetric measurements were performed by a computerized Electrochemical Trace Analyzer Model 273A-PAR (Princeton Applied Research, Oak Ridge, TN, USA) controlled via 270/250 PAR software was used for the cyclic voltammetry measurements. The electrode assembly (Model 303A- PAR) incorporating of a micro-electrolysis cell of a three electrode system comprising of a hanging mercury drop electrode as a working electrode (area: 0.026 cm^{-1}), an $Ag/AgCl/KCl_s$ reference electrode and a platinum wire counter electrode, was used. Stirring of the solution in the micro-electrolysis cell was performed using a magnetic stirrer (305 - PAR) to provide the convective transport during the pre-concentration step. The whole measurements were automated and controlled through the programming capacity of the apparatus. The supporting electrolyte used was 0.1 M n-Bu_4NClO_4. The solvents used were sufficiently pure and the concentration of the complexes was 0.001 M.

2.5. Oxidase biomimetic catalytic activity (catechol oxidase and phenoxazinone synthase)

A mixture of 1.0 ml of studied substrate 3,5-di-tert-buty1catehol (3,5-$DTBCH_2$) or o-aminophenol (OAPH) solution (30 mM) in methanol and 1.0 ml of copper complex solution (~3 mM) in methanol was placed in a 1 cm path length optical cell containing 1.0 ml of methanol in a spectrophotometer. The final concentration of reaction mixture is catechol or o-aminophenol (10 mM) and complex (l mM). The formation of 3,5-di-tert-butyl-quinone (3,5-DTBQ) was followed by observing the increase of characteristic quinone absorption band at 400 nm and for 2-amino-3H-phenoxazine-3-one (APX) at 433 nm. For each set of observation, a curve of concentration of 3,5-DTBQ or APX formed (calculated by using the corresponding ε value) versus time was plotted and initial rates were calculated by drawing a tangent to curve at t = 0 and finding its slope. After this initial fast phase, the average rate of reaction was also calculated. The above described experiment was repeated under two sets: i) in the reaction mixture the concentration of catalyst was varied (0.5, 1.0, 2.0 mM) and concentration of 3,5-$DTBCH_2$ or OAPH was kept constant at 20 mM. ii) Concentration of 3,5-$DTBCH_2$ or OAPH was varied (10, 20, 30, 40 mM) and concentration of catalyst was kept fixed at 1.0 mM. For each set of data initial rates were calculated and graphs of rate versus concentration of catalyst and rate versus concentration of both catechol and o-aminophenol were plotted.

2.6. Kinetic Experiments

Kinetic measurements were studied on KinetAsyst SF-61DX2 stopped-flow instrument coupled to an online data acquisition system. The spectral changes of the reactions were first recorded over the wavelength range of 190-600 nm to establish a suitable wavelength at which the kinetic trace could be followed. The wavelengths used for each reaction are listed above. The catalytic reactions were studied under pseudo first order conditions. This was achieved by using at least a 10-fold excess of the studied substrates. All reported rate constants represent an average value of at least three independent kinetic runs for each experimental condition.

3. Results and Discussion

3.1 Synthesis and characterization of copper(II) complexes **1-4**

A new diimine–Schiff base ligands containing a donor sets of N_3S_2, or N_2S_2 and their mononuclear copper(II) complexes were prepared via applying template synthesis technique by treating an ethanolic solution of $CuCl_2$ with the Schiff-bases which were formed in situ. A template condensation of two moles of 4-amino-6-methyl-5-oxo-3-(2H)-thioxo-1,2,4-triazine and one mole of 2,6-pyridine dicarbaldehyde or the appropriate α- dicarbonyl in the presence of one mole of copper(II) salt ($CuCl_2$ $2H_2O$) in absolute ethanol gave good yields of the analytically pure products of a series of mononuclear copper(II) complexes with N_3S_2 or N_2S_2 donors containing pentadentate (L^1) or tetradentate (L^2, L^3 and L^4) diimine Schiff-base ligands. In the absence of the template metal ion, predominately polymeric or oligomeric products were obtained. This fact reflects that the metal ion directs the condensation reaction preferentially towards the favorable ligand molecule rather than the oligomeric or polymeric product.

These newly synthesized copper(II) complexes are non-hygroscopic in nature and stable as solids or in solution under the atmospheric conditions. They are colored microcrystalline solids and their color being various shades of green. They are insoluble in common organic solvents viz. ethanol, chloroform, benzene, cyclohexane, acetone, diethyl ether, etc., but are freely soluble in MeOH, DMF and DMSO. The complexes are neutral with the metal charge entirely neutralized by the doubly deprotonated Schiff-base ligands. In spite of all the effort, none of these copper(II) complexes could be crystallized for their single crystal X-ray diffraction studies.

10^{-3} M solutions of the complexes in DMF at room temperature show low molar conductance values (26.8–45.2 Ω^{-1} mol^{-1} cm^2) and indicate that they are non-electrolytes (Gray 1971). The elemental analysis results are in a close agreement with the calculated values for the proposed molecular formulae of these copper(II) chelates. Thus, on the basis of the elemental analyses, and the molar conductance measurements the complexes were assigned the compositions shown in Table 1.

Table 1. Molecular formulae, physical properties and elemental analytical data of copper(II) complexes **1-4**

Complex	Color	Λ_M ($\Omega^{-1}cm^2$ mol^{-1})	Found (calcd.) C	H	N	M
$[CuL^1 H_2O]H_2O$	Faint green	33.30	35.30 (34.99)	2.73 (3.30)	24.39 (24.48)	12.69 (12.34)
$[CuL^2 H_2O]$	Faint green	45.20	32.63 (32.17)	3.54 (3.57)	25.24 (25.03)	14.55 (14.19)
$[CuL^3 H_2O]H_2O$	Green	36.80	32.85 (32.53)	3.27 (3.33)	23.16 (23.35)	13.79 (13.24)
$[CuL^4 H_2O]H_2O$	Olive green	26.80	44.62 (44.36)	4.20 (4.00)	17.14 (17.24)	9.98 (09.77)

3.2 Thermal analysis

3.2.1. Thermal decomposition (TGA and DTG)

Thermal decomposition studies on the synthesized copper(II) complexes **1** – **4** have been carried out so as to corroborate the information obtained from their molar conductance and spectral studies about the statues of water molecules present in these complexes, as well as to know their general decomposition patterns. The thermogravimetric analysis was carried out in N_2 atmosphere from the ambient temperature up to 1100 °C. The

calculated weight losses percentage were estimated based on the TG data and agree quit well with the suggested molecular formulae of the investigated complexes.

Table 2. Thermogravimetric analysis degradation of copper(II) complexes **1-4**

Complex	Temperature °C	DTG_{max} °C	Weight loss Found (calcd.)	Species formed
$[CuL^1(H_2O)]\ H_2O$	70 - 100	80	3.12(3.30)	$[CuLH_2O]$
	195 – 250	200	31.25(31.4 9)	$[CuL_{(0.65)}]$
	250 – 1100	900	51.50(52.38)	CuO
$[CuL^2(H_2O)]$	160 – 210	200	3.90(04.04)	[CuL]
	210 – 340	280	15.40 (16.26)	$[CuL_{(0.80)}]$
	340 – 700	600	19.40(20.33)	$[CuL_{(0.55)}]$
	700 –1000	800	41.30(42.26)	CuO
$[CuL^3(H_2O)]\ H_2O$	75 – 110	95	3.95(4.7590)	$[CuLH_2O]$
	250 – 340	310	3.71(4.7590)	[CuL]
	340 – 500	430	19.15(19.780)	$[CuL_{(0.75)}]$
	500 – 700	-	57.15(57.37)	CuO
$[CuL^4(H_2O)]\ H_2O$	75 – 130	85	2.50(2.77)	$[CuLH_2O]$
	150 – 220	210	2.30(2.77)	[CuL]
	220 – 350	290	38.84(39.78)	$[CuL_{(0.53)}]$
	350 – 450	440	44.41(44.88)	CuO

The decomposition stages, temperature ranges, maximum decomposition peak DTG_{max}, percentage mass losses of the decomposition reactions together with their theoretical percentage mass losses and the assignments of decomposition moieties are given in Table 2 which revealed the following findings:

The thermogram of the hydrated copper(II) complex **2**, exhibits two stages of thermal pyrolysis within the temperature range 160 - 1000 °C. The first stage shows the dehydration process which starts at 160 °C and comes end at 200 °C. The weight loss is corresponding to the volatilization of the axially coordinate water molecule. Since the decomposition started above 160 °C the presence of any surface or crystalline solvent/water molecules may be ruled out. The second thermal degradation step starts at 200 °C and ends at 820 °C and comprises several successive and unresolved steps, with the maximum decomposition peaks DTG_{max} at 280, 600 and 800 °C. The corresponding mass loses are due to the complete decomposition and removal of the organic portion. The mass loss in this stage is in a good agreement with calculated mass loss and the final product is quantitatively proved to be anhydrous metallic oxide.

The TG and DTG curves of complexes **1**, **3** and **4** show that, these complexes have a similar decomposition patterns. From the thermograms it can be observed that, the three complexes decompose in three to four successive overlapped and unresolved degradation stages.

The first stage of thermal decomposition starts at 70 °C and is marked with a regular loss in mass up to 130 °C. The initial mass loss for these complexes varies from 2.50 to 3.95 %, obtained in initial pyrolysis process and agrees well with the theoretical expected loss of 2.77 – 4.76 %. This is mainly due to the dehydrate removal of the out sphere water molecules (the adsorbed, crystalline or lattice water). The maximum rate of mass loss occurs within temperature range of 80 - 95 °C as indicated by the DTG_{max} peaks. The activation energy value of this thermal dehydration step is lying in the range 48.17 – 90.4500 kJ mol^{-1} (Table 3). This ease of desolvation suggests the weak interaction of water; i. e. water plays little or no role in the lattice forces and occupies crystal voids.

The second stage of mass-loss reveals that the hydrated intermediates are then further decomposed within the temperature range 150 –340 °C, with DTG maximum at 200, 310 and 210 °C for (**1**), (**3**) and (**4**) respectively. This process corresponds to the volatilization of the axially coordinated water molecule and the energy value of activation lies in the range 42.08 – 184.01 kJ mol^{-1} (Table 3). Concerning complex **1** the second stage describes to the explosion of the coordinate water molecule is overlapped with next thermal pyrolysis process and a significant sharp weight loss was observed due to the partial decomposition of the organic ligand molecule.

The third and fourth thermal pyrolysis stages of complexes (**3**) and (**4**) and the final stage for complex (**1)** involve a significant mass loss extending from 250 to 1100 °C with DTG maximum at the temperature rang of 440 - 900 °C corresponding to the partial decomposition of the organic ligand molecule in successive steps, leaving behind metal oxide as the final product of the thermal pyrolysis of the complex molecule. The activation energy values lie in the ranges 52.27 – 66.63 and 108.92 – 132.96 kJ $mol^{-1}$of the third and fourth thermal degradation stages respectively. Further horizontal constant curve observed for complex (**4)** may be due to the presence of metal oxides residue in the remaining part.

The total mass loss of the various decomposition stages are 85.87, 83.96 and 88.05 %, for complexes **1**, **3** and **4** respectively leaving metal oxide (CuO) as a residue. The metal content, determined from the oxide residue, was found to be satisfactory agreement with values calculated on the basis of the suggested composition formulae based on the elemental analysis data. In the final degradation stage of complexes **1**, **3** and **4** there is a correlation between the calculated and the experimental weight losses.

3.2.2. Thermal Kinetic Studies

All the well characterized decomposition stages of the synthesized copper(II) complexes(**1**) – (**4**) were selected for the study of the kinetics of decomposition. The thermodynamic parameters of the decomposition processes namely, activation energy ($E_a^{\#}$), enthalpy ($\Delta H^{\#}$), entropy ($\Delta S^{\#}$), and Gibbs free energy change ($\Delta G^{\#}$) were evaluated graphically by employing the Coats-Redfern (Coats et al., 1964) equation. The values of various kinetic parameters calculated are given in (Table 3).

Table 3. Kinetic and thermodynamic parameters of copper(II) complexes **1** – **4**

***Complex**	**T° (K)**	***A***	***E_a***	**ΔH**	**ΔS**	**ΔG**
1	0516	10.19	064.30	061.38	-0.2384	184.43
	0565	35.33	184.01	181.10	-0.2880	310.42
	0838	0.698	048.77	045.86	-0.2648	267.76
2	0465	27.75	122.18	119.26	-0.2292	225.87
	0616	0.165	027.91	024.99	-0.2741	193.89
	0689	13.32	103.83	100.92	-0.2386	265.35
	0966	14.94	058.74	055.82	-0.2213	269.61
3	0425	19.86	048.14	045.23	-0.2120	135.36
	0507	24.49	077.17	074.25	-0.2310	191.38
	0723	15.92	052.27	049.35	-0.2375	221.11
	0930	23.98	132.96	130.04	-0.2362	349.76
4	376	25.22	090.45	087.53	-0.2283	173.37
	463	06.20	042.08	039.16	-0.2417	151.07
	598	08.25	066.63	063.71	-0.2414	208.10
	698	27.17	108.92	178.00	-0.2328	340.52

*Complex details are as listed in Table 1. E_a, ΔH and ΔG are in kJ mol^{-1}, ΔS in J mol^{-1}.

The activation energies (E_a) in the different stages of thermal decomposition of the investigated complexes are in the range of 48.77 – 122.18 kJ mol^{-1}. The corresponding values of the pre-exponential factor (A) of the different thermal degradation stages are in the range of 10.19 –25.22 s^{-1}. The respective values of the entropy of activation (ΔS) are in the range of -23.84×10^2 to -21.20×10^2 J mol^{-1}. Neither the values of A nor the values of ΔS show a definite trend along the series, but the energy of activation for the second-stage decomposition is almost higher than that of the first stage.

The data in Table 3 show that the activation energy E_a and ΔG values of the first stage of decomposition of the hexacoordinated [CuL^1] and the five coordinated complexes [CuL^3] are lower than of the five coordinated complexes [CuL^2] and [CuL^4]. This may be ascribed to the structural rigidity of the [CuL^2] and [CuL^4] complex molecules as compared to [CuL^1] and [CuL^3] complexes. On the other hand, on comparing the activation energy and ΔG values of the second stage of decomposition of the complexes [CuL^1], [CuL^3], [CuL^2] and [CuL^4], the latter two

complex species, [CuL^2] and [CuL^4], show remarkably lower values. This may be due to the less steric strain for the intermediate compound formed for [CuL^2] and [CuL^4] complexes compared to the other complexes.

For all complexes, in most thermal degradation steps the values of ΔG increase for the subsequently decomposition stages due to increasing the values of TΔS from one step to another which override the value of ΔH. This increase reflects that the rate of the subsequent removal of the organic ligand portion will be lower than that of the precedent ligand. This may be ascribed to the structural rigidity of the remaining complex after the explosion of the coordinated water molecule, as compared with precedent complex, which require more energy for its rearrangement before undergoing any compositional change. The positive values of ΔH (Table 3) means that the thermal decomposition processes are endothermic. The negative value of ΔS observed of all complexes, (Table 3) indicates that the activated complexes have more ordered structure than the reactants.

3.3. Mode of bonding

The IR spectra of the free components of the in suit synthesized Schiff base ligands and their corresponding copper(II) complexes were compared to get information about the coordination behavior of these ligands with copper(II) ion. It was noted that a pair of bands are present in the spectrum of the free (uncomplexed and uncondensed) 4-amino-6-methyl-5-oxo-3-(2H)-thioxo-1,2,4-triazine moiety, at 3400 and 1610 cm^{-1} corresponding to $\upsilon(NH_2)$ group which are absent in the spectra of all synthesized copper(II) chalets. The disappearance of these bands which are characteristic for the free primary ammine moiety (~3400 cm^{-1}) suggests that the Schiff condensation had occurred. The appearance of a new, strong intensity, band in the region 1585–1592 cm^{-1}, attributed to the characteristic stretching frequencies of the linkage ν(C=N) (Nakamoto 1970; Chandra 2005) provides strong evidence in favor of the formation of Schiff base ligand system. The data in (Table 4) display that frequency value of the υ(C=N) is lower than that usually found for the azomethine linkage (Silverstein et al., 1981). This lower value of υ(C=N) stretching energy may explained on the basis of a drift of the loin pair density of the azomethine nitrogen towards the copper(II) central atom (Ilham et al., 2007; Lopaez-Carriga et al., 1986) indicating that the coordination takes place through the nitrogen atom of the (C=N) group. This contention finds support in the presence of new bands in the spectra of the complexes at 2920, 1370, 1190 and 680 cm^{-1} characteristic to the aliphatic dicarbonyl moieties and assignable to $\upsilon(CH_3)$, $\delta(sym.CH_3)$, $\upsilon(C\text{-}CH_3)$, δ(C-H) and ring deformations respectively. Concerning, the imine complexes derived from α-dicarbonyl, the spectra reveal an absorption band in the region 1200 - 1220 cm^{-1} characteristic to the α-diimine moiety of the metal chelates (Rai et al., 1994). This finding has observed in several α-diimine containing tetraaza macrocyclic Schiff–base complexes (Maroney et al., 1984). Thus, it appears that each α- diketone or 2,6-pyridine dicarbaldehyde molecule has reacted with the amino groups of the two molecules of 4-amino-6-methyl-5-oxo-3-(2H)-thioxo-1,2,4-triazine forming the tetradentate Schiff-base copper(II) complex molecule. This behavior is analogous to the fact that one diketone molecule reacts with two available amine groups, forming ring closer and giving rise to macrocyclic metal complex molecule (Maroney et al., 1984). On the other hand the spectrum of the free 4-amino-6-methyl-5-oxo-3-(2H)-thioxo-1,2,4-triazine characteristic bands due to υ(NH) and υ(SH) at 3145 and 2700 cm^{-1} respectively (Nakamoto 1986) and another band at 1047 cm^{-1} assigned to υ(C=S) (Singh et al., 2007). These observations suggest that the free 4-amino-6-methyl-5-oxo-3-(2H)-thioxo-1,2,4-triazine exhibits thiole-thione toutomerism. The important feature common to all complexes is the occurrence of new absorption bands at the ranges 744 – 763 and 405 – 412 cm^{-1} attributed to the υ(C-S) and υ(M-S) vibrations, respectively (El-Shazly et al., 2005; Kumar et al., 2002). This finding suggests ligand enothiolization followed by the thiol proton loss during the chelation with the metal ion. This observation supports the formation of M-S bond via deprotonation of the thiol group (S-H) and the coordination via thiolate sulfur is inferred from the absence of the υ(C=S) vibration with the simultaneous appearance of new bands due υ(C–S) and υ(M–S) vibrations. The IR spectrum of the free 4-amino-6-methyl-5-oxo-3-(2H)-thioxo-1,2,4-triazine shows also sharp band of strong intensity at about 1700 cm^{-1} assigned as υ(C=O). In the metal complexes, this band occurs either at the same wave number as in the free 4-amino-6-methyl-5-oxo-3-(2H)-thioxo-1,2,4-triazine or at slightly shifted wave number, indicating the non-involvement of the carbonyl oxygen of C=O group in coordination to copper(II) center.

Coordination of the pyridine nitrogen to copper(II) ion is inferred from the observation that, the $\upsilon(C=N)_{py}$ stretching mode band of the Schiff base ligand (L^3) in the spectrum of the copper(II) complex [CuL^3] is recorded at 1572 cm^{-1} and this band is at approximately 25 cm^{-1} higher wave numbers than in the free 2,6-pyridine dicarbaldehyde, as a result of the coordination of copper(II) to pyridine nitrogen. The bonding of the pyridine nitrogen atom is also supported by the presence of medium bands at 1030 cm^{-1} and 668 cm^{-1} attributable to the ring breathing frequency and the low energy pyridine ring vibrations, respectively (Radecka-Paryzek et al., 1998).

All these above data suggest the following facts: (i) Schiff base ligand derived from 2,6-pyridine dicarbaldehyde (L^3) is dibasic pentadentate ligand coordinated to the copper(II) ion via the two deprotonated thiolate

sulfurs and the nitrogens of the Schiff-base linkages in addition to the pyridine nitrogen. (ii) Schiff base ligands, (L^2, L^3 and L^4), derived from the other α- dicarbonyls, are dibasic tetradentate ligands coordinated to the copper(II) ion through the two deprotonated thiolate sulfurs, and the azomethine nitrogen atoms.

All the complexes show bands at around 3290 – 3430 cm^{-1} suggesting the presence of water molecules in them. The thermogravimetric analysis suggests the presence of two molecules of water per molecule of the complexes. The presence of the coordinated water in complexes is inferred from the observed weak bands detectable at 854-920 cm^{-1}, which may be assigned to the rocking and wagging modes.

The IR spectra of these newly synthesized copper(II) Schiff base complexes also show non-ligand bands in the ranges 461 – 495 cm^{-1} and 443 – 475 cm^{-1}, which are tentatively assigned to υ(M–N) and υ(M–S), respectively.

Table 4. Infra red spectra of copper(II) complexes **1-4**

Complex	υ(H_2O)	υ(C=N)	υ(C-S)	δ(H_2O)	υ(N-Cu)	υ(S-Cu)
[CuL^1H_2O]	3467	1610	748	933	462	414
[CuL^2H_2O]	3450	1602	748	933	458	410
[CuL^3H_2O] H_2O	3448	1608,1592	746	935	460	412
[CuL^4H_2O] H_2O	3436	1598	748	937	460	403

3.4. Electronic absorption spectra

The electronic absorption spectra of the free 4-amino-6-methyl-5-oxo-3-(2H)-thioxo-1,2,4-triazine in addition to the synthesized copper(II) complexes 1-4 were measured at room temperature in DMF solution and the corresponding data for the copper(II) complexes are given in Table 5. The electronic absorption spectrum of the free 4-amino-6-methyl-5-oxo-3-(2H)-thioxo-1,2,4-triazine shows absorption band in the high energy region attributed to $\pi \rightarrow \pi^*$ of the carbonyl group of this compound (Silverstein et al., 1981; Ramadan 1997). This band exhibits no significant change in the spectra of all complexes, confirming the non-participation of the carbonyl oxygen atom of the 4-amino-6-methyl-5-oxo-3-(2H)-thioxo-1,2,4-triazine moiety in the complexation. The strong absorption band in the 27027 - 37037 cm^{-1} range of all complexes originating from the azomethine linkage of the Schiff-base moiety, and it is assignable: $n \rightarrow \pi^*$ (West et al., 1998; 1991).

Regarding the five coordinate copper(II) complexes (**2**), (**3**) and (**4**) the position and intensity of $n \rightarrow \pi^*$ band originating from the azomethine linkage show dependence on the nature of the substituents within the carbonyl imine moiety of the tetradentate Schiff–base ligands. An examination of λ_{max} values (Table 5) for $n \rightarrow \pi^*$ indicates that an electron donating alkyl group e.g. CH_3 and CH_2CH_3 increases the λ_{max} value while an electron-withdrawing group e.g. phenyl ring decreases it. This is obvious as the electron density around the copper(II) center is higher in the presence of electron donating group and the reverse is true when an electron-withdrawing group is present. As a result of this, the charge transfer $n \rightarrow \pi^*$ transition requires higher energy for the former and lower energy for the latter. For analogous copper(II) Schiff-bases the Lewis acidity of the central copper(II) show dependence on the energy value of the c. t. $n \rightarrow \pi^*$ of the azomethine group (C=N) (West et al., 1995). The increasing order of this energy **3** > **2** > **4** reflects the decreasing order of the Lewis acidity of the copper(II) center. On contrast, the conjugation effect of the phenyl group induces red shift in the $n \rightarrow \pi^*$ transition of the Schiff-base linkage. Thus the Lewis acidity as shown by the c. t., $n \rightarrow \pi^*$ band energy increases in the order **4** > **2** > **3**.

As shown in Table 5, the electronic absorption spectral data for the five – coordinated complex species **2**, **3**, and **4** are all similar. Three weak peaks appearing in the low energy visible region at 14175 –14513, 16129 – 16528 and 17123 – 18975 cm^{-1} ranges may be attributed to the d-d transitions of the copper(II) ion in the square-pyramidal environment (C_{4v}) (Lever 1984). In the square – pyramidal copper(II) complexes the plausible d-orbital energy level scheme (idealized symmetry group C_{4v}), is $dx^2–y^2 > dz^2 > d_{xy} > d_{xz}, d_{yz}$. Accordingly, for complexes, **2**, **3**, and **4** the higher energy band of the d-d transitions can be assigned to $d_{xz}, d_{yz} \rightarrow dx^2–y^2$, $d_{xy} \rightarrow dx^2–y^2$ and the lower energy band to $dz^2 \rightarrow dx^2–y^2$. These spectral parameters are in consistence with the other monomeric copper(II) complexes in the five-coordinate square-pyramidal stereochemistry (Onawumi et al., 2008; Patel et al., 2007; El-Metwaly 2006). This finding is further confirmed from the results of the ESR spectra.

The uv electronic absorption spectrum of the free 2,6-pyridine dicarbaldehyde gives rise to high energy absorption band below 300 nm, due to the pyridine $\pi \rightarrow \pi^*$ transition (Selmeczi et al., 2003). Concerning the hexa-coordinated pyridine based copper(II) complex **1**, the electronic absorption spectral data in Table 5 show that there is a significant change in the energy of $\pi \rightarrow \pi^*$ on complexation. The band maximum originating from the pyridine $\pi \rightarrow \pi^*$ transition in the spectrum of this chelate is shifted to lower frequencies relative to those in the free 2,6-

pyridine dicarbaldehyde. This bathchromic shift may result from the extended conjugation in the ligand system forced by the chelated metal ion (Ismail et al., 1997) and confirms the participation of pyridine nitrogen in the complex formation. In the low energy region the spectrum of complex **1** shows weak electronic absorption bands at 13513, 18518 and 20833 cm^{-1} which may be assigned to the transitions, $^2B_{1g} \rightarrow {}^2B_{2g}$ (υ_1), $^2B_{1g} \rightarrow {}^2A_{1g}$ (υ_2) and $^2B_{1g} \rightarrow {}^2E_g$ (υ_3) suggesting a tetragonally distorted octahedral geometry (Lever 1984).

For all complexes the uv – absorption spectra display the intra-ligand bands in the high energy regions at 27185 – 29761 and 34013 – 37313 cm^{-1} corresponding to the n → π* and π → π* transitions, respectively, and a strong S → Cu^{II} charge-transfer band in the 26041 – 28089 cm^{-1} range. The presence of a S → Cu^{II} (LMCT) band in the electronic spectra of these complexes further supports bonding of the ligands to copper(II) ion via the thiolate sulfur atoms. The presence of a S → Cu^{II} (LMCT) band is quite common in the electronic spectra of copper(II) complexes containing sulfur donors ligands (Akbar et al., 1996; Bingham et al., 1987).

Table 5: Electronic absorption spectra of copper(II) complexes **1** - **4**

*Complex	λ(cm^{-1}) $^2B_{1g} \longrightarrow {}^2A_{1g}$	$^2B_{1g} \longrightarrow {}^2B_{2g}$	$^2B_{1g} \longrightarrow {}^2E_g$	S → Cu^{II}	n → π*	π → π*
1	13513 $dz^2 \rightarrow dx^2–y^2$	18518 $d_{xy} \rightarrow dx^2–y^2$	20833 $d_{xz}, d_{yz} \rightarrow dx^2–y^2$	27777	28487	37313
2	14285	16422	17988	27027	28289	34282
3	14513	16528	18975	28089	29761	34846
4	14175	16129	17123	26041	27185	34013

*Complex details are as listed in Table 1

3.5. EPR spectra and magnetic moment measurements

The effective magnetic moments (BM) of the investigated copper(II) complexes were measured at room temperature and the results obtained are recorded in Table 6 which demonstrate that the present copper(II) Schiff base complexes are magnetically dilute. The observed magnetic moments fall in the range 1.94 – 2.15 BM and indicate the monomeric nature of the complexes. These values are close to the spin only (S=1/2) behavior of 1.73 B.M. for d^9 configuration and reflects the absence of any metal-metal interaction with the neighboring molecules. This finding is further confirmed from the clear resolution of the ESR spectra. The reported magnetic moment values correspond to one unpaired electron indicating the complexes may be considered as tetragonal geometry.

The X-band ESR spectra of the polycrystalline samples of the reported copper(II) complexes **1** –**4** were recorded at frequency 9.1 GHz under the magnetic field strength 3100 G scan rate 1000 recorded at room temperature. The polycrystalline EPR spectra of the five coordinated copper(II) complexes **2**, **3** and **4** under study are almost similar and the simulation of the obtained spectra indicates three different principal values of g, showing that the copper(II) ion in these five-coordinated complexes is in a rhombically distorted ligand field with EPR parameters deduced from the simulated one, $g_1 = 2.01$, $g_2 = 2.13$ and $g_3 = 2.27$. For systems where $g_3 > g_2 > g_1$, the ratio $R = (g_3 – g_2)/(g_2 – g_1)$ indicates the ground state of the complex (El-Shazly et al., 1980). If $R > 1$, the ground state is predominantly dz^2 while the ground state is predominantly $dx^2–y^2$ when $R < 1$. The value of R for the present five – coordinated complexes is less than one and as a consequence the unpaired electron is in the $dx^2–y^2$ orbital. This agrees with the electronic absorption results which suggest the coordination around copper(II) is a highly distorted square-pyramidal geometry. Concerning complex **4**, the ratio R is 0.99, and as this value is higher than that of the other analogous complexes **2** and **3** and close to R = 1 we can propose a highly distorted square pyramidal arrangement of copper(II) for the complex (**4)**.

The EPR spectrum of the hexa-coordinate copper(II) complex (**1)** shows an axial type signal with the $g_{\|}$ values occurring higher than those for $g_{\perp}$. Both $g_{\|}$ and $g_{\perp}$ values are within the range expected for the tetragonal distorted octahedral copper(II) complexes. The observed trend $g_{\|} > g_{\perp} > 2.0023$, indicates that the unpaired electron lies predominantly in $dx^2–y^2$ orbital, giving $^2B_{1g}$ as the ground state (Bose et al., 2000; Ray et al., 1990; Hathaway et al., 1970). The g_{av} values were calculated using the relation; $g_{av} = 1/3(g_{\|} + 2g_{\perp})$. For the five coordinate complex species (**2)**, (**3)** and (**4)** the low field region of spectra gives $g_3 = 2.245$ which was taken as $g_{\|}$. Also, for these complexes the high field region of spectra is resolved into g_1 and g_2 components, $g_2 = 2.0309$, and $g_1 = 1.9966$, and $g_{\perp}$ was

calculated as $g_{\perp} = 1/2(g_x + g_y)$. This may result as a consequence of the non-equivalence of the CuN_2S_2 bonds formed in the XY plane (Sreekanth et al., 2003).

The EPR parameter G has been calculated by using the expression (Hathaway et al., 1970): $G = (g_{\parallel} - 2)/(g_{\perp} - 2)$. The value of G reflects the exchange interaction between copper centers in the polycrystalline solid complexes. According to Hathaway et al. (Hathaway et al., 1970; 1968) values of G less than 4 indicate considerable exchange interaction in the solid complexes while values of G larger than 4 are typical of negligible exchange interactions, which is the case in the copper(II) complexes under investigation. The average g values (Table 6) are found to be in the range 2.084 – 2.230, i. e. above the free ion value (2.0023) which indicates strong covalency in bonding between the copper(II) ion and the ligand molecule (Fidone et al., 1959).

Table 6. ESR spectral parameters and magnetic moment values of copper(II) complexes **1** - **4**

Complex	g_3 ($g_{\parallel}$)	g_2	g_1 ($g_{\perp}$)	R	g_{av}	G	μ_{eff} (BM)
$[CuL^1Cl]Cl$	2.466	-	2.113	-	2.230	4.124	1.81
$[CuL^2]H_2O$	2.584	2.321	1.846 (2.084)	0.554	2.084	6.990	1.92
$[CuL^3H_2O]H_2O$	2.451	2.241	1.870 (2.055)	0.566	2.187	8.200	1.84
$[CuL^4H_2O]H_2O$	2.518	2.256	1.922 (2.072)	0.993	2.220	7.472	1.83

Thus, on the basis of above discussion which is based upon elemental analysis, molar conductance, magnetic susceptibility, IR, electronic, EPR spectral studies and thermal analysis (TGA & DTG); the suggested structures of the reported copper(II) **1** –**4** complexes are given in Scheme 1.

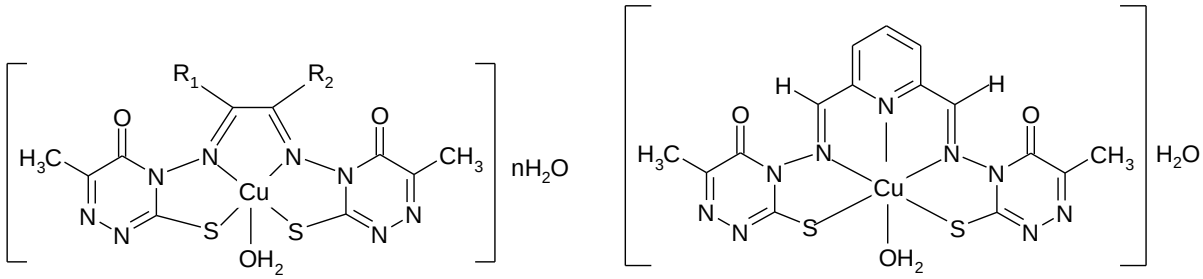

(**2**) $R_1 = R_2 = CH_3$; n = 0

(**3**) $R_1 = CH_3$; $R_2 = CH_2CH_3$; n = 1

(**4**) $R_1 = R_2 =$ 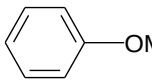 ; n = 1

(**1**)

Scheme 1. Structure of copper(II) complexes **1** - **4**

3. 6. Electrochemical properties

Electrochemistry and coordination chemistry overlap in many important areas of fundamental and technological interest. Particularly for copper complexes, because some copper(II) complexes can serve as models for redox enzymes such as catechol oxidase and phenoxazinone synthase. The electrochemistry of the complexes (**1) – (4)** was investigated, as the redox potential is an important parameter in electron transfer processes in general and also in our catalytic systems. The redox potentials of the catalysts and species involved in the redox cycles have to match some criteria. The redox potential should be such as to permit the reoxidation of the reduced copper(I) centers by

molecular oxygen to maintain the catalytic cycle. The reduction of copper(II) by the substrates, 3,5-di-tert-butylcatechol or 2-aminophenol, and the reoxidation of copper(I) by dioxygen are significant steps in the catalytic cycle. The redox potentials of the complexes **1**, **2**, **3** and **4** were measured by cyclic voltammetry (CV) at a working platinum electrode in methanol solution containing 0.1 M tetra butyl ammonium perchlorate (TBAP) as the supporting electrolyte in the range of -1.5 to 1.5 V versus AgCl/Ag. The cyclic voltammetric data are given in Table 7, and a representative cyclic voltammogram of the reported copper(II) complexes is shown in Figure 1.

The electrochemical data, in Table 7 along with the magnetic results previously described, establish that the complexes exist as a monomer. The reduced forms of complexes **1** – **4** all display reasonable chemical stability on the time-scale of the cyclic voltammetry experiment. Cyclic voltammograms of the entire complexes exhibit a reversible oxidation and reversible reduction peaks at the scan rate 100 mV s^{-1}. All the complexes showed well-defined waves in the range ($E_{1/2}$) 0.376 to 0.606 V of the couple (Cu^{II}/Cu^{I}) versus Ag/AgCl. The redox processes are reversible with peak-to-peak separation (ΔE_p) values ranging from 59 to 65 mV. However, the value of the limiting peak-to-peak separation (ΔE_p), which lies within the normal values for a reversible one – electron redox process suggests that the heterogeneous electron – transfer process in these complexes is easily reversible (ΔE_p, 60 mV for a reversible one - electron redox process) (Brown et al.,1971) and not accompanied by stereochemical reorganization (Karlin et al., 1980). The peak potentials separation and the ratio of cathodic to anodic peak current are close to unity consistent with one-electron process. This indicates that the electron transfer is reversible and the mass transfer is limited. The electrode processes can be described by the following equation; $[CuL^{II}] + e \rightleftharpoons [CuL^{I}]$.

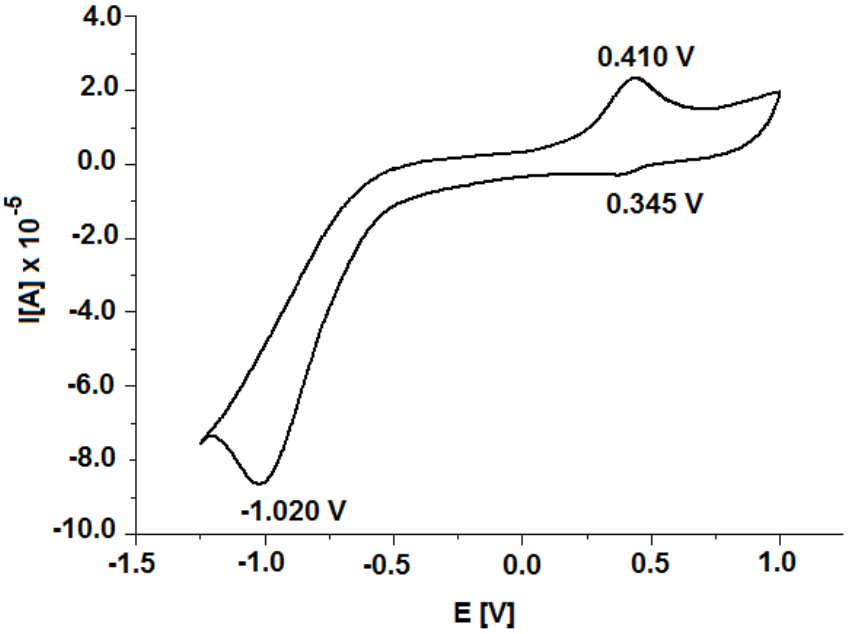

Figure 1. Cyclic voltammogram of complex **4** (0.001M) in DMF (scan rate 100 mV/s) with 0.1 tetrabutylammonium hexa-fluorophoshate (TBAH) as supporting electrolyte at 295 K. The reference electrode was Ag/AgCl

The data in Table 7 reveal that the nature of substitution on the Schiff- base linkage has a significant effect on $E_{1/2}$ of the reported complexes. The electron-withdrawing groups stabilize the lower oxidation state Cu^{I} in the complex [CuL^4] while the electron-donating group favors oxidation to CuL^{II} in the complexes [CuL^2] and [CuL^3]. This is possibly because the electron-withdrawing phenyl ring makes the complex more positively charged and hence causes it to be more easily reduced. Similarly the electron-donating groups as inductive or mesomeric alkyl make the complexes [CuL^2] and [CuL^3] less positively charged and hence less easily reduced. On the other hand the data in Table 7 demonstrated that, the difference in the redox potential values of complexes **1** - **4** is strongly related to the basicity of the donor atoms of the coordination environment around the central copper(II) ion. The coordination chromophore of complexes **2**, **3** and **4** is N_2S_2 while for complex **1** is N_3S_2, and the later comprises the more basic pyridine nitrogen donor. Thus, complexes formed with coordination chromophore has higher electron density (basicity) will show higher redox ($E_{1/2}$) values than that formed with coordination chromophore has lower electron density. The fact that the reduction is completely reversible indicates that the reported proposed six – and

five-coordinate geometries are stable in both oxidation states, at least on the cyclic voltammetry time scale. The redox potential value (0.376 V) of complex **4** however, does not differ greatly than the reported value of +360 mV versus SCE for the enzyme tyrosinase isolated from mushrooms (Makino et al., 1974). The impact of the electrochemical properties on the catalytic reactivity of these complexes will be discussed below.

Table 7. Electrochemical data of the copper(II) complexes **1-4**

Complex*	E_{pc}	E_{pa}	ΔE_p/mV	$E_{½}$/V	i_c/i_a
1	0.575	0.638	63	o.606	0.96
2	0.443	0.502	59	0.472	1.12
3	0.578	0.515	63	0.546	1.10
4	0.410	0.345	65	0.376	1.40

*Complex details are as listed in Table 1, (scan rate of 100 V/s).

3.7. Catalytic studies

3.7.1. Catechol oxidase biomimetic catalytic activity

The oxidase biomimetic catalytic activity of the present copper(II) complexes towards the aerobic oxidation of 3,5-di-tert-butylcatechole (3,5-DTBCH$_2$) under catalytic conditions was studied using electronic spectroscopy by following the appearance of the absorption maximum of the 3,5-di-tert-butylquinone (3,5DTBQ) at 400 nm over time. Some of the obtained results are illustrated in Figure 2, showing the change in absorbance at 400 nm versus time for the first 30 min. No other oxidation products could be detected.

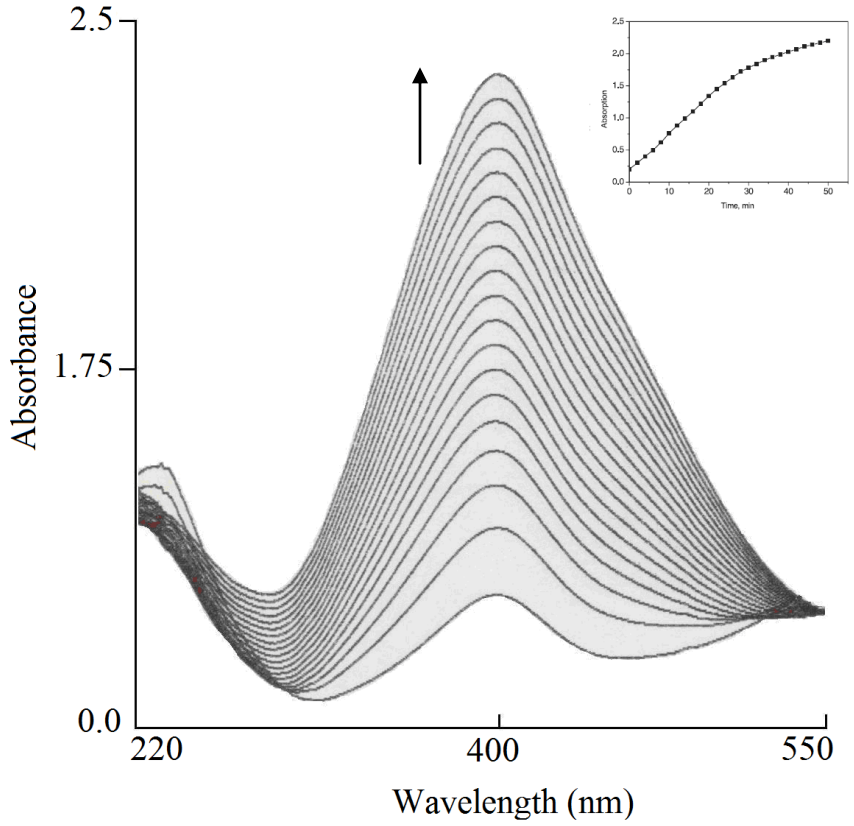

Fig. 2. Monitoring the increase in the characteristic 3,5-di-*tert*-butylquinone absorption band at 400 nm as a function of time.

3.7.1.1. Kinetic measurements

The kinetic measurements on the oxidation of 3,5-DTBCH$_2$ were carried out by the method of initial rates by monitoring the increase in the characteristic quinone (3,5-DTBQ) absorption band at 400 nm as a function of time.

The reactivity studies were performed in methanol solution at ambient conditions. In order to determine the rate dependence on the concentration of the various reactants namely catalyst and substrate runs were performed at different concentrations of these reactants.

Carrying out the kinetic experiments by varying the concentration of the studied complexes and keeping the concentration of 3,5-DTBCH$_2$ constant, a first – order dependence was found. The data in Figure 3 show the effect of catalyst concentration on the rate constant k_{obs} of the oxidation reaction. The rate constant k_{obs} increased linearly with increasing catalyst concentration.

At ambient temperature and atmospheric oxygen pressure, when the complexes were treated with varying concentrations of 3,5-DTBCH$_2$, a first-order dependence on the 3,5-DTBCH$_2$ concentration was observed at low concentrations. However, at higher 3,5-DTBCH$_2$ concentrations, the complexes **1-4** showed saturation kinetics. This indicates that an intermediate complex-substrate adduct forms in a preequilibrium process and that the irreversible substrate oxidation is the rate – determining step of the catalytic cycle. A treatment on the basis of the Michaelis-Menten model, therefore, seemed appropriate. Lineweaver-Burk (Figure 4, double reciprocal) plots for **1-4** gave reasonable straight lines, from which the parameters such as maximum velocity V_{max}, rate constant for the dissociation of the complex- substrate intermediate (the turnover number) (k_{cat}), Michaelis binding constant K_M and the constant k_{cat}/K_m which measures the catalytic efficiency were evaluated. A representative plot is shown in Figure 3. The results evaluated from Lineweaver-Burk plots presented in Table 8 and demonstrate that, the catalytic activities depend strongly on the nature of both the ligand substituents within the carbonyl moiety and the junction between the central nitrogen donors of the azomethine linkages of the in situ formed diimine ligands.

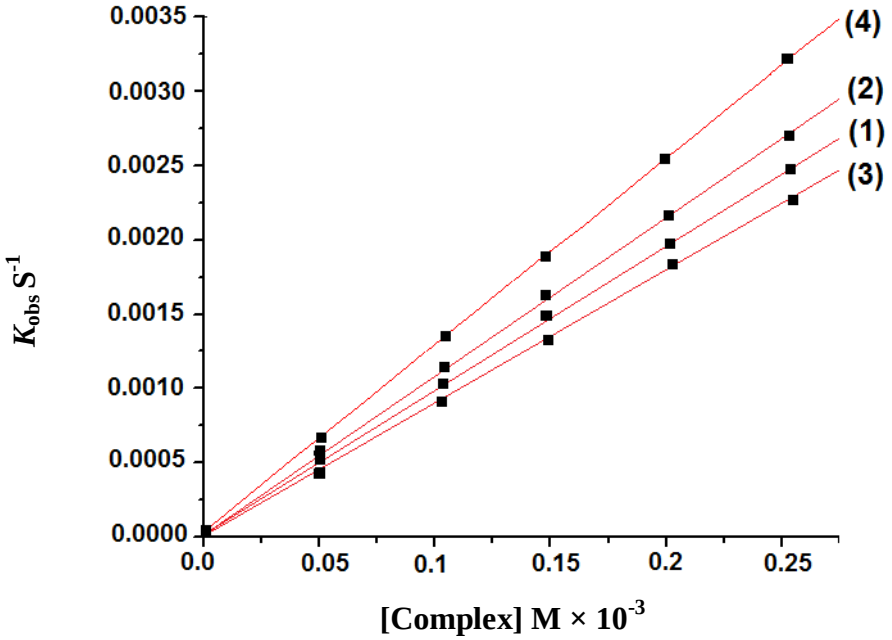

Fig. 3. The rate constant k_{obs} dependence on the concentration of complex **1-4**. Conditions: [complex] = 0.5 × 10^{-4} – 2.5 × 10^{-4} M, [TEA] = 0.001 M, [3,5-DTBC] = 0.5 × 10^{-4} M, T=25 ˚C, in air.

The results evaluated from Linewevear-Burk plots are V_{max} = 22.0 × 10^{-3}- 125.0 × 10^{-3} M s^{-1}, K_M = 14.3 × 10^{-3} 330.0× 10^{-3} M, k_{cat} = 8.8 - 500.0 s^{-1} and k_{cat} / K_M =3.52 × 10^2 - 15.16 × 10^2. By comparison these results with other catechol oxidase model systems of mononuclear copper(II) complexes (Kupan et al., 2009) the present copper(II) complexes show moderate catechol oxidase biomimetic catalytic activity but significantly lower than those reported for the binuclear copper(II) complexes (k_{cat} = 200 – 6000) and at least many orders of magnitude less than the natural enzyme (k_{cat} = 8250) (Smith et al., 2008). On the basis of the k_{cat} values above, and by comparison with other binuclear copper(II) complexes (Smith et al., 2008) it can be said that the binuclear copper(II) complexes show higher catechol oxidase like catalytic activity than the mononuclear complexes due to the fact that this kind of mechanism requires two metal ions in close proximity.

Table 8. The kinetic parameter of the catalytic oxidation of 3,5-DTBC

*Complex	V_{max} M s^{-1}	K_M M	k_{cat} s^{-1}	k_{cat}/K_M M^{-1} s^{-1}	$TR \times 10^{-3}$ h^{-1}	$**TR \times 10^{-3}$ h^{-1}
1	29.5×10^{-3}	14.3×10^{-3}	11.80	8.25×10^{2}	12.70	75.98
2	35.0×10^{-3}	24.0×10^{-3}	14.00	5.83×10^{2}	17.98	69.75
3	22.0×10^{-3}	25.0×10^{-3}	8.80	3.52×10^{2}	6.54	42.17
4	125.0×10^{-3}	330.0×10^{-3}	500.0	15.16×10^{2}	32.96	98.66

*Complexes details are as listed in Table 1; [Complex] = 2.5×10^{-4}: ** these data were obtained in presence of TEA; (TR = amount of 3,5-DTBQ produced per min per mg of catalyst)

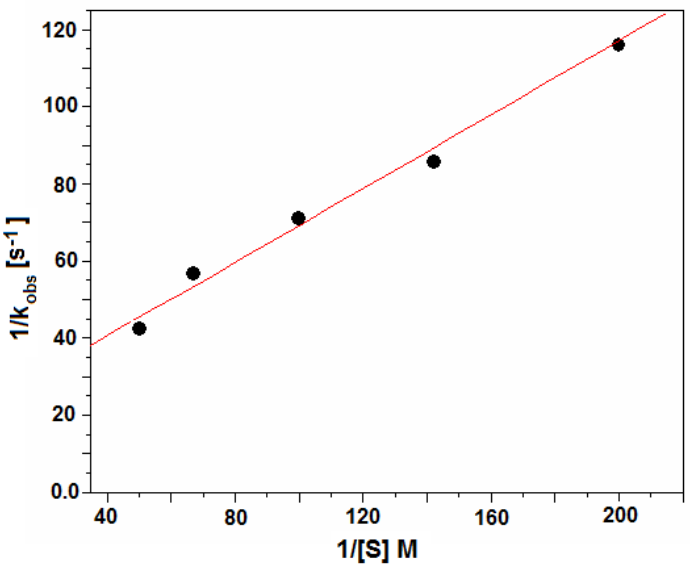

Fig. 4. Lineweaver – Burk plot of 3,5-DTBC oxidation by complex **1**. Conditions: [3,5-DTBC] = 0.5×10^{-2} – 2.0×10^{-2} M, [TEA] = 1.0×10^{-3} M, [complex] = 0.5×10^{-4} M, T=25 °C, in air.

Importance is the comparison of the reactivity of CuL^4 with the other reported copper(II) complexes CuL^1, CuL^2 and CuL^3 displayed much superior activity than CuL^1, CuL^2 and CuL^3. The higher catalytic activity observed for CuL^4 complex, is probably due to the conjugation effect of the phenyl group in L^4. The presence of the conjugation in this complex renders it stronger in the studied oxidation reaction.

The moderate to low catechol oxidase like catalytic activity for CuL^1, CuL^2 and CuL^3 respectively, are attributed to a number of factors which need to be considered in explaining the differences in the catechol oxidase like catalytic activity of the titled complexes and these factors will be considered sequentially.

4.7.1.2. Basicity of the donor atoms

The catalytic investigations of reported copper(II) complexes with L^2, L^3 and L^4 suggest that their reactivity is dependent on the Lewis basicity of the donor nitrogens of the imine ligand created by the nature of substituents on the carbon atom of the Schiff base linkage of these diimine ligands. It has been previously reported that the nature of the donor atoms, the counter ion, or any bridging group bound to the metal centers has an effect on the rate of catalysis (Voldeba et al., 1989; Solomon et al., 1992). In addition, it has been shown that electron transfer from catechol to LM^{n+} can begin only after catechol and the LM^{n+} species form a LM^{n+}- catecholate intermediate (Rogic et al., 1983). Accordingly, the initiation step almost certainly involves production of copper(I) by the interaction of copper(II) complex with catechol. In this situation, the Cu^{+}/Cu^{2+} couple is involved as a redox center. According to the mechanistic hypothesis, the Lewis acidity of the copper(II) center in the copper(II)-catecholate intermediate greatly affects the redox potential of the Cu^{+}/Cu^{2+} couple and consequently the degree of the catalytic reactivity. Thus, an increase in the Lewis acidity of a copper(II) center in the $[(CuL^n)_2$-catecholae] complex facilitates electron transfer from the catecholate ring to the copper(II) center. For CuL^2, CuL^3 and CuL^4 complexes, the electronic

absorption spectra exhibit a charge transfer band assignable to n → π* of the azomethine linkage of the diimine ligand. The position and intensity of this band show dependence on the type of substituents within the carbonyl moiety of these diimines. The increasing order of this energy ($CuL^3 > CuL^2 > CuL^4$) reflects the decreasing order of the Lewis acidity of the copper(II) center (Ramadan et al., 2005; Karlin et al., 1985; Cox et al., 1988). The presence of the electron-donating alkyl group CH_3, and CH_2CH_3, in L^2 and L^3 respectively increases the Lewis basicity of the donor nitrogen atoms and shifts the charge transfer n → π* band of the C=N to higher energy (Table 5). In contrast, the conjugation effect of the phenyl group in L^4 induces a red shift in the n → π* band of the azomethine linkage. Thus, the Lewis acidity of copper(II) center of these copper(II) chelates, as shown by the c.t. n → π* band energy, increases in the order: $CuL^3 < CuL^2 < CuL^4$. Consequently, in the [$(CuL^n)_2$-catecholate] intermediate, electron transfer from the catecholate ring to the CuL^4 center is assumed to be more favored as compared with CuL^2 and CuL^3 complexes. These data are consistent with the premise that the basicity of the donor atoms is one of the primary factors in modulating the resultant electrochemical properties of the complexes.

4.7.1.3. Electrochemical Considerations.

In the oxidation of catechol to quinone the initiation step implies that the copper(II) ion is reduced to copper(I) and subsequent reoxidation to copper(II) during the oxidation process. The redox potentials ($E_{1/2}$) of complexes **1-4** have been obtained in order to determine if there is a correlation between the $E_{1/2}$ of these complexes and the rate of oxidation of 3,5-di-tert-butylcatechol. Several studies have shown previously that electrochemical potentials play a marked role in determining the reactivity properties of copper(II) complexes (Malachowski et al., 1989; 1995; 1998; 1996; 1992).

It should be noted that the enzyme tyrosinase catalyzes the aerobic oxidation of catechol to the light absorbing o-quinone isolated from mushroom (Agaricus bisporus) has a reported value for E° of 0.36 V vs. the standard calomel reference [65]. It is obvious however, that the enzyme has been able to balance successfully the requirements of the different oxidation states of the metal: $M^{n+} \rightleftharpoons M^{(n-1)+}$ in performing its catalytic tasks. The balance between ease of reduction of copper(II) and subsequent reoxidation copper(I) by molecular oxygen must be maintained for efficient catalysis to occur. This would imply that a window of $E_{1/2}$ values exists wherein effective catalysis can take place. If the reduction potential is too negative, reduction to copper(I) be unattainable; on the other hand, if the reduction potential is too positive, the catalytic cycle would be short-circuited because once reduced to copper(I), the complexes would be unable to be easily reoxidized to copper(II) by O_2.

Concerning the pyridine based copper(II) complex CuL^1, the electronic absorption spectral data in Table 5 show that the band maximum originating from the pyridine π → π* transition in the spectrum of this chelate is shifted to lower frequencies relative to those in the free 2,6-pyridine dicarbaldehyde. This bathchromic shift may result from the extended conjugation in the ligand system forced by the chelated metal ion. The presence of the conjugation in this complex (rich in electron and stability) renders it strong catalyst in the studied oxidation reaction. The greater catalytic activity of **4** compared to **1** can be correlated with their redox potentials. $E_{½}$ of **4** (0.376 V) approaches the reported $E_{½}$ value of the natural enzyme. On the other hand complex **1** exhibits $E_{1/2}$ value of 0.606 V that deviate from that potential and consequently this leads to significant loss of activity. This finding suggests that, within a certain range of $E_{1/2}$ values appreciable catalysis is possible, while outside that range the drop off in rate is quite significant.

4.7.1.4. Effect of Lewis-base (Et_3N)

Triethylamine (TEA) was added to the oxidation reaction medium in order to investigate the effect of added base on the reactivity experiments. When TEA was added to a solution in which the copper(II)-catalyzed oxidation of 3,5-$DTBCH_2$ a remarkable increase ca. three to six fold was found in the oxidation rate. There is a kinetic factor, which account for this dramatic increase of the catalytic activity on addition of TEA. On the basis of the results above we believe that the first step in the catalytic cycle is the formation of the [-3,5-DTBC-$(CuL)_2$] species, which takes place via deprotonation and binding of 3,5-$DTBC^{2-}$. In methanol solution 3,5-di-tert-butylcatechol (3,5-$DTBCH_2$) is mainly present in its diprotonated form 3,5-$DTBCH_2$. Due to the presence of Lewis-base in the reaction medium, catechol may be predominantly present in the monoprotonated form (3,5-$DTBCH^-$) or the non-protonated 3,5-$DTBC^{2-}$. The kinetic activity of 3,5-$DTBCH^-$ or 3,5-$DTBC^{2-}$ presumably is the spark for initiation of the oxidation catalytic cycle. Previous studies of metal chelates which catalyze the oxidation of catechol have been demonstrated that the catechol species interacting with the catalyst is the catecholate anion i. e. 3,5-$DTBCH^-$ or 3,5-$DTBC^{2-}$ (Tyson et al., 1972; Waite et al., 1976).

4.7.1.5. Probable catalytic sequence

Based on the above kinetic and catalytic investigations a probable catalytic reaction sequence can be represented as follow:

$3,5\text{-DTBC} + 2[Cu^{II}LX] \rightleftharpoons [3,5\text{-DTBC} - (Cu^{II}L)_2] + 2HX$ (1)

$[3,5\text{-DTBC} - (Cu^{II}L)_2] \rightarrow 2[Cu^{I}L] + 3,5\text{-DTBQ}$ (2)

$2[Cu^{I}L] + O_2 \rightarrow [(Cu^{II}L)_2O_2]$ (3)

$3,5\text{-DTBC} + [(Cu^{II}L)_2O_2] \rightarrow [3,5\text{-DTBC} - (Cu^{II}L)_2O_2] + 2H^+$ (4)

$[3,5\text{-DTBC} - (Cu^{II}L)_2O_2] + 2H^+ \rightarrow [3,5\text{-DTBC} - (Cu^{II}L)_2(OH)_2]$ (5)

$[3,5\text{-DTBC} - (Cu^{II}L)_2(OH)_2] + 2HX \rightarrow 3,5\text{-DTBQ} + 2[Cu^{II}LX] + 2H_2O$ (6)

For the synthesized copper(II) complexes **1**-**4**, we believe that the non-protonated catecholate anion $DTBC^{2-}$ first binds to tow molecules of the catalyst in a reversible pre-equilibrium step (Eq. 1). The produced [catecholate-$(Cu^{II}L)_2$] intermediate oxidizes the coordinated catecholate anion ($3,5\text{-}DTBC^{2-}$) in a fast reaction step to the corresponding light absorbing o-quinone (3.5-DTBQ) and forming the copper(I) species ($Cu^{I}L$) (Eq. 2). Tow molecules of this copper(I) complex then react in a reversible reaction with dioxygen in a slow, rate-determining step to the copper dioxygen complex $[(Cu^{II}L)_2O_2]$ (Eq. 3). $[(Cu^{II}L)_2O_2]$ reacts then with $DTBCH_2$ in a fast reaction steps (Eq. 4-6) to give the products DTBQ and two molecules of H_2O and the catalyst is regenerated in its original active form in closing up the catalytic cycle.

3.7.2. Phenoxazinone synthase biomimetic catalytic activity

Related to catechol oxidase biomimetic catalytic activity is the ability of the reported copper(II) complexes to promote the oxidation of 2-aminophenol (OAPH) to 2-amino-3H-phenoxazine- 3-ones (APX) as shown in Scheme 2.

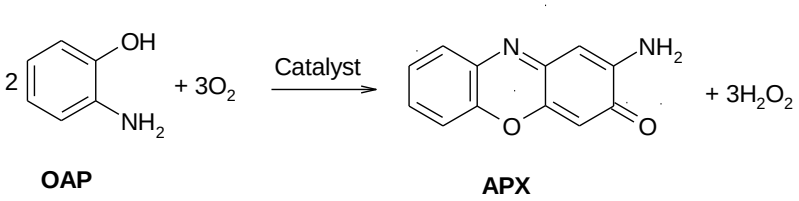

Scheme 2: Aerobic catalytic oxidation of 2-aminophenol

In order to investigate the phenoxazinone synthase biomimetic catalytic activity of the synthesized copper(II) complexes the reaction of o-aminophenol (OAPH) with dioxygen in presence of catalytic amount of the titled complexes $[Cu^{II}L^n]$ was studied. The complexes were suitable catalysts for the model reaction according to Scheme 2, and the main products of the reaction were 2-amino-3H-phenoxazin-3-one (APX) and H_2O_2. No significant decomposition of the formed H_2O_2 could be observed and the reaction between the APX and the peroxide is negligible. The reactivity studies were performed in methanol solution at room temperature. Before proceeding into the detailed kinetic study, we need to check the ability of our copper(II) complexes to catalyze the oxidation of OAPH to the light absorbing APX. For this purpose, 1×10^{-4} mol L^{-1} solutions in methanol of complexes **1**–**4** were treated with 1×10^{-2} mol L^{-1} (100 equivalents) of OAPH at room temperature under aerobic condition. The course of the reaction was studied using electronic spectroscopy by following the appearance of the absorption maximum of APX at 433 nm over time as shown in Figure 5 as a representative of catalytic aerobic oxidation of OAPH.

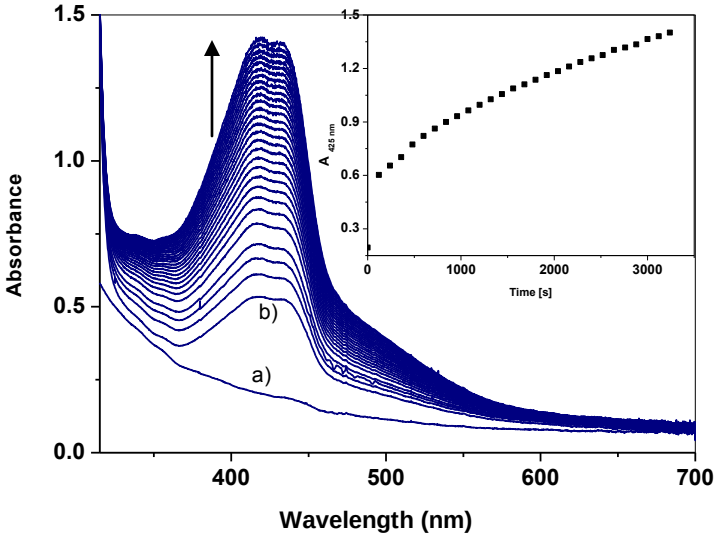

Figure 5. UV/Vis spectral changes recorded for the reaction of complex **3** with 2-aminophenol (0.5×10^{-1} M) in methanol at 296 K; (a) spectrum before the reaction; (b) spectrum obtained several milliseconds after mixing of the reactants in the stopped-flow; inset is the kinetic trace at 433 nm

3.7.2.1. Kinetic studies

The kinetic studies were carried out under pseudo-first-order conditions and runs were conducted by measuring the 2-amino-3H-phenoxazin-3-one formed during the reactions and on that base the initial reaction rates were calculated.

3.7.2.1.1. Dependence of rate on catalyst concentration

The dependence of the reaction rate on the catalyst concentration is illustrated in Figure 6 at constant concentration of both OAPH and O_2. In presence of variable amounts of catalyst, the initial rate is linearly dependent on the catalyst concentration. These kinetic measurements of the reaction rate with respect to the catalyst concentration indicate first-order dependence. As the curves in Figure 6 pass through the origin, i.e. without intercept, it can be stated that there is no measurable rate of oxidation in the absence of the catalyst.

3.7.2.1.2. Dependence of rate on substrate concentration

To determine the dependence of the rate on the substrate concentration, solutions of the complexes **1-4** were treated with increasing amounts of OAPH. Kinetic measurements of the reaction rate with respect to the 2-aminophenol concentration reveal first-order dependence at low concentration of substrate. Under these experimental conditions, and at higher concentration of OAPH, saturation kinetics was found for the initial rates versus the concentrations of OAPH (Figure 7).

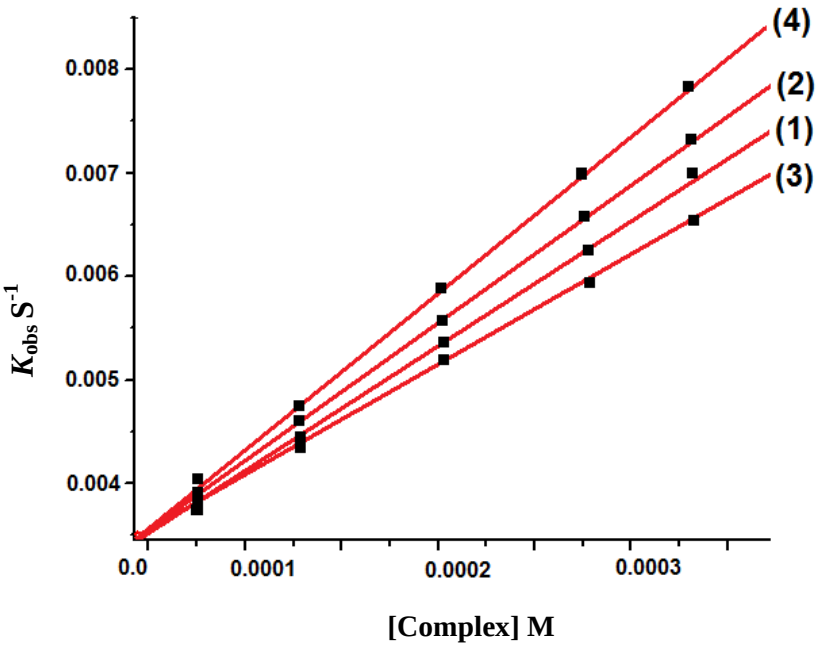

Fig. 6. The rate constant k_{obs} dependence on the concentration of complexes **1**-**4**. Conditions: [complex] = 5×10^{-5} – 4×10^{-4} M; [OAPH] = 0.01 M, T=25 ˚C, in air.

This indicates that an intermediate complex-substrate adducts forms in a pre-equilibrium process and that the irreversible substrate oxidation is the rate-determining step of the catalytic cycle in a great similarity with that reported above for catechol oxidation. An analysis of the data based on the Michaelis–Menten model, originally developed for enzyme kinetics, was applied. The results evaluated from Line weaver–Burk plots, V_{max} M s^{-1}, K_M M, k_{cat} s^{-1} and k_{cat}/K_M M^{-1} s^{-1} for complexes **1**, **2**, **3** and **4** are given in Table 9.

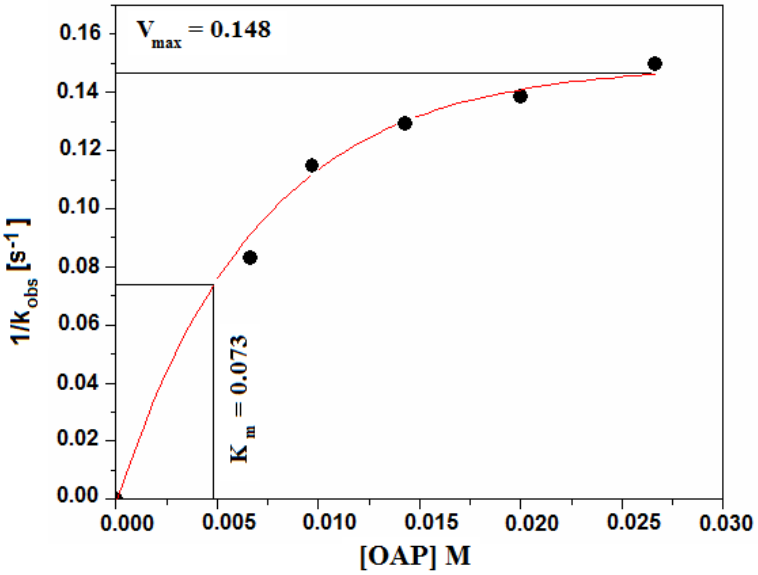

Fig. 7. The rate constant, k_{obs} dependence on the concentration of OAPH for complex **1**. Conditions: [OAPH] = 5×10^{-3} – 3×10^{-2} M; [complex] =2.5×10^{-4} M, T=25 ˚C, in air.

On the basis of k_{cat}/K_M values (Table 9), the catalytic efficiency of the investigated copper(II) complexes have the order **4** > **2** > **1** > **3** as was observed above for catechol oxidation. Accordingly, this trend in the catalytic reactivity of these copper(II) complexes **1**-**4** can be attributed to the same rezones discussed above for catechol oxidation. The

molar absorbance value 2.33×10^4 M^{-1} cm^{-1} of the APX (Golub et al., 1972) was used to determine the concentration of APX formed and consequently calculation the turnover rate. The calculated turnover rates of 14.54 – 62.96 h^{-1} are higher than those above calculated for the catechol oxidation (6.54 -32.96 h^{-1}). As well as, the data in Tables 7 and 8 reveal that the present copper(II) complexes exhibit lower oxidase catalytic efficiency towards the aerobic oxidation of 3,5-$DTBCH_2$ as compared to that reported for OAPH. Comparing the K_M values which measure the substrate's affinity towards the present copper(II) complexes it is observed that under identical experimental conditions 3,5-$DTBCH_2$ has lower affinity than OAPH. This means that the complex–aminophenolate, [OAP-$Cu^{II}L]^+$, binding is stronger than that in case of the complex–catecholate, [3,5-DTBC-$(CuL)_2$], but the rate of formation of quinone is smaller than that APX production.

Table 9. The kinetic parameter of the catalytic oxidation of *o*-aminophenol

*Complex	V_{max} M s^{-1}	K_M M	k_{cat} s^{-1}	k_{cat}/K_M M^{-1} s^{-1}	$TR \times 10^{-3}$ h^{-1}	$**TR \times 10^{-3}$ h^{-1}
1	48.0×10^{-3}	29.0×10^{-4}	19.2	66.20×10^2	32.70	124.98
2	73.0×10^{-3}	46.0×10^{-4}	29.2	63.47×10^2	27.98	119.75
3	29.0×10^{-3}	48.0×10^{-4}	11.6	24.16×10^2	14.54	52.17
4	148.0×10^{-3}	733.0×10^{-4}	592.0	81.09×10^2	62.96	181.66

*Complexes details are as listed in Table 1; [Complex] = 2.5×10^{-4} M; ** these data were obtained in presence of TEA; (TR = amount of APX produced per min per mg of catalyst)

3.7.2.1.3. Probable mechanism

A mechanism for the reaction catalyzed by the native phenoxazinone synthase (PHS) in S. antibiotics has been proposed (Barry, et al., 1989) where the o-aminophenol is first oxidized by two electrons to the quinone imine, which then conjugates to a second o-aminophenol molecule while still bound to the enzyme. This product is further oxidized by two electrons to give rise to the p-quinone imine. The last two steps of the reaction, another conjugation to generate the tricyclic structure and a final two-electron oxidation to yield the 2-aminophenoxazinone product, are thought to be non-enzymatic (Barry, et al., 1989). The mechanism of this complex six-electron oxidation was determined by using a variety of substituted o-aminophenols designed to block the reaction at intermediate stages (Barry, et al., 1989).

Similar to that reported previously (Barry, et al., 1989) and on the basis of our kinetic data, a reaction mechanism as outlined in Scheme 3 is proposed. According to this proposed mechanism, the o-aminophenolate monoanion (OAP^-) first binds to the copper(II) center of [$Cu^{II}L$] in a reversible pre-equilibrium, and thereafter the forming of aminophenolate-copper(II), [H_2OAP-$Cu^{II}L$], adduct. In this intermediate the substrate 2-aminophenolate (H_2OAP^-) may coordinate to copper(II) center in a bidentate fashion. The resulting [H_2OAP-$Cu^{II}L$] intermediate could then reorganize under intermolecular electron-transfer to the $M^{(n-1)+}$ center and the semioxidized o-aminosemiquinone (o-ASQ), which remains coordinated to the copper(I) center. According to the electro-neutrality principal, this intermediate is highly unstable because the greater Lewis-basicity of (o-ASQ) leads to excessive build-up of electron density on the copper(I) center, rendering it susceptible to O_2 attack. Consequently it reacts with the dioxygen in a further equilibrium step and upon O_2 binding to copper(I) center, a redox reaction occurs involving the transfer of an electron to oxygen molecule from the copper(I) ion, leading to reduction of O_2 to produce the superoxide anion radical ($O_2^{\bullet-}$) giving copper(II) superoxide complex. This redox interaction has been postulated in several mechanistic Schemes describing the role of the metal ion in the catalytic oxidation of organic substrates (Ramadan et al., 2005, 2006, 2011, 2012; and references their in). The resulting dioxygen adduct undergoes via intramolecular hydrogen abstraction from the vicinal primary amino group to bound $O_2^{\bullet-}$ to produce the perhydroxide radical ($HO_2^{\bullet}$) in the rate-determining step. Such rearrangement is perfectly possible, considering the proximity of primary amino group to $O_2^{\bullet-}$ that exist in the activated intermediate complex [o-ASQ-CuL-$O_2^{\bullet-}$]. As consequence of this rearrangement, electron transfer from the o-aminosemiquinone ring provides the oxidized form o-benzoquinone monoimine (o-BQMI) and hydroperoxide fragment bound to copper(II) center. In a fast reaction, electrophilic attack by a proton on the oxygen of the perhydroxide radical ($HO_2^{\bullet}$) bonded to copper(II) yields o-BQMI and H_2O_2 as a by-product, via disproportionation of o-ASQ and $HO_2^{\bullet}$ giving the starting copper(II) complex just to close up the reaction cycle.

The previous studies demonstrated that (o-BQMI) is the precursor to the (APX) formation and its further conversation into the product (APX) can be rationalized by the reaction described in the references (Zaki et al., 2000; Kaizer et al., 2008) and showed in (Scheme 3). The overall reaction requires several oxidative dehydrogenation steps involving (OAP, O_2) and o-benzoquinone monoimine as reactants on the way to (APX).

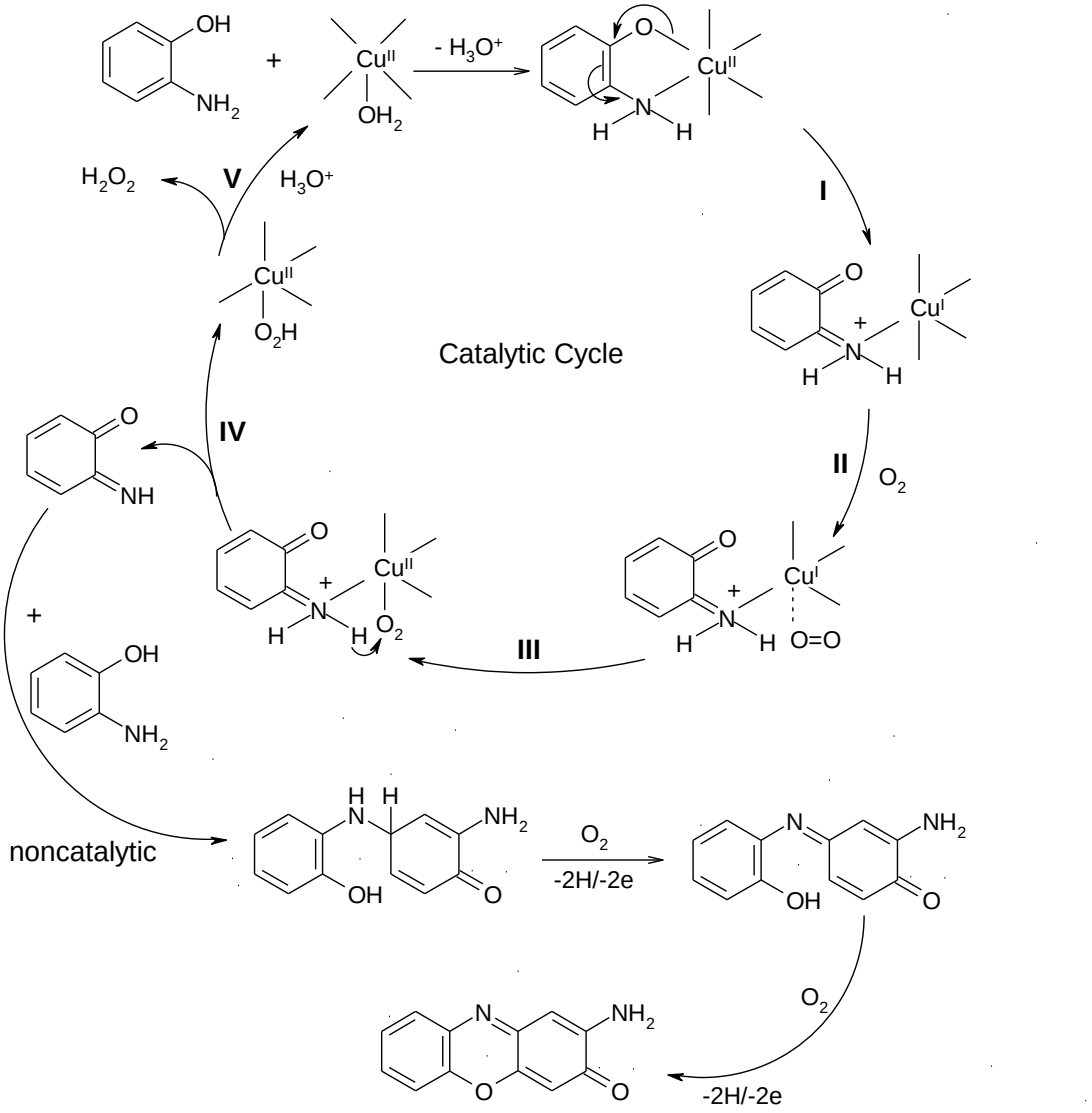

Scheme 3. Catalytic aerobic oxidation cycle of 2-aminophenol

3.7.2.1.4. Effect of Lewis-base (Et_3N)

Similar to the catechol-containing systems the effect of the TEA (triethylamine) base was also investigated. When TEA was added to a solution in which the copper(II) catalyzed oxidation of 2-aminophenol was in progress, a much more dramatic increase (ca. 2.88 – 4.28 fold) was found in the oxidation rate. In methanol solution o-aminophenol is mainly present in its protonated form OAPH. Due to the presence of TEA in the reaction medium, o-aminophenol may be predominantly present in the non-protonated form OAP^-. In analogous to catechol the kinetic activity of OAP^- presumably is the spark for initiation of the oxidation catalytic cycle. Previous studies of metal chelates which catalyze the oxidation of catechol have been demonstrated that the phenol species interacting with the catalyst is the phenolate anion (Tyson et al., 1972; Waite et al., 1976). In this case the TEA deprotonates OAPH to OAP^-, which binds to catalyst, yield a $[OAP\text{-}Cu^{II}L]^+$ species analogous to that generated in the case of the catechol containing system. The resulting $[OAP\text{-}Cu^{II}L]^+$ intermediate could then reorganize under intermolecular electron-transfer to the copper(II) center and the semioxidized o-aminosemiquinone (o-ASQ), which remains coordinated to the copper(I) center. Then this intermediate binds to O_2 resulting in the formation of the superoxide

o-ASQ-$Cu^{II}L$ intermediate, which decomposes in the rate-determining step, yielding BQMI and $Cu^{II}L$ in its original active form.

Conclusion

A new series of diimine–Schiff base ligands containing sulfur and nitrogen donor sets and their mononuclear copper(II) complexes were prepared via applying template synthesis technique. The structural characterization was achieved based upon analytical and spectroscopic investigations. The complexes are neutral with the metal charge entirely neutralized by the doubly deprotonated two thiolate sulfurs of the Schiff-base ligands. The copper(II) centers of these complexes show different coordination numbers and stereochemistries. Catalytic investigations demonstrated that the title complexes are able to catalyze the aerobic oxidation of 3,5-di-tert-butylcatechol (3,5-$DTBCH_2$) to the respective light absorbing 3,5-di-tert-butyl-benzoquinone (3,5-DTBQ). Related to catechol oxidase biomimetic catalytic activity is the ability of these oxidase models to promote the oxidative coupling of 2-aminophenol (OAPH) to 2-aminophenoxazine-3-one (APX) which means that the present copper(II) complexes serve as good functional models for catechol oxidase and phenoxazinone synthase enzymes. Kinetic measurements revealed first order dependence on the catalyst concentration and saturation type behavior with respect to the corresponding substrate. From the obtained results, it is also found that the catalytic activity of the investigated copper(II) complexes towards the oxidation of 2-aminophenol is higher than that of catechol oxidation. In addition to the former the catalytic reactivity seems to be markedly dependent on the Lewis acidity of copper(II) center created by ligand substituents within the carbonyl moiety. On the basis of k_{cat}/K_M values, the catalytic efficiency of the title complexes has the order **4** > **2** > **1** > **3** for both systems catechol oxidase and phenoxazinone synthase like activity. On the basis of kinetic data plausible mechanisms were proposed for both systems assuming ternary complex formation between catalyst, substrate and dioxygen, in which the latter one is the rate-determining step. It was also found that the added triethylamine in both systems greatly accelerates the reaction.

References

Holm, R.H., Solomon, E.I., Chem. Rev. **2004**, 104, 347.
Harrop, T.C., Mascharak, P.K., Acc. Chem. Res. **2004,** 37, 253.
Lobana, T.S., Isobe, K. H., Kitayama, Nishioka, T., Kinoshita, I., Angew. Chem., Int. Engl. **2004**, 43, 213.
Sellmann, D., Prakash, R., Heinemann, F.W., Eur. J. Inorg. Chem. **2004,** 1847.
Reddy, P.A.N., Santra, B.K., Nethaji, M., Chakravarty, A.R., J. Inorg. Biochem. **2004,** 98, 377.
Dhar, S., Senapati, D., Das, P.K., Chattopadhyay, P., Nethaji, M., Chakravarty, A.R.,. J. Am. Chem. Soc. **2003,** 125, 12118.
Santra, B.K., Reddy, P.A.N., Nethaji, M., Chakravarty, A.R., J. Chem. Soc., Dalton Trans. **2001,** 3553.
Holm, R.H., Kennepohl, P., Solomon, E.I., Chem. Rev. **1996**, 96, 2239.
Ali, M. A., Hossain, S. M. G., Majumder, S. M. M. H., Nazimuddin, M., Tarafder, M.T.H., Polyhedron **1987,** 6, 1653.
Minkel, D.T., Saryan, A.L., Petering, D.H., Cancer Res. **1978,** 38, 124.
Minkel, D.T., Chanstier, C.H., Petering, D.H.,. Mol. Pharmacol. **1976,** 12, 1036.
Minkel, D.T Chanstier, C.H., Petering, D.H., Bioinorg. Chem. **1976,** 5, 203.
Ronson, T.K., Adams, H., Ward, M.D., Cryst. Eng. Commun. **2006,** 8, 497.
Tavacoli, S., Miller, T.A., Paul, R.L., Jeffery, J.C., Ward, M.D., Polyhedron **2003,** 22, 507.
Argent, S.P., Adams, H., Riis-Johannessen, T., Jeffery, J.C., Harding, L.P., Clegg, W., Harrington, R.W., Ward, M.D., Dalton Trans. **2006,** 4996.
Xie, Y.B., Li, J.R., Bu, X.H., Polyhedron **2005,** 24, 413.
Gennari, M., Lanfranchi, M., Cammi, R., Pellinghelli, M.A., Marchio, L.,. Inorg. Chem. **2007,** 46, 10143.
Wang, H., Li, M.X., Shao, M., He, X., Polyhedron **2007,** 26, 5171.
Ganesamoorthy, C., Balakrishna, M.S., George, P.P., Mague, J.T., Inorg. Chem. **2007,** 46, 848.
Liaw, B. J., Lobana, T.S., Lin, Y.W., Wang, J.C., Liu, C.W., Inorg. Chem. **2007,** 44, 9921.
Barry, C.E., Nayar, P.G., Begley, T.P., Biochemistry **1989,** 28, 6323.
Jones, G.H., Hopwood, D.A.,. J. Biol. Chem. **1984,** 259, 14151.
Barry, C.E., Nayar, P., Begley, T.P., 1988. J. Am. Chem. Soc. 110, 3333.
Homma, M., Graham, A.F., Biochim. Biophys. Acta **1962,** 61, 642.
Katz, E., Weissbach, H., J. Biol. Chem. **1962,** 237, 882.
Prati, L., Rossi, M., Ravasio, N., J. Mol. Catal. **1992,** 79, 347.
Horvath, T., Kaizer, J., Speier, G., J. Mol. Catal. A–Chem. **2004,** 215, 9.

Szeverenyi, Z., Milaeva, E.R., Simandi, L.I., J. Mol. Catal. **1991,** 67, 251.
Simandi, L.I., Barna, T., Korecz, L., Rockenbauer, A., Tetrahedron Lett. **1993,** 34, 717.
Simandi, L.I., Barna, T., Nemeth, S., J. Chem. Soc. Dalton Trans. **1996**473.
Simandi, T.M., Simandi, L.I., Gyor, M., Rockenbauer, A., Gomory, A., Dalton Trans. **2004,** 1056.
Simandi, T.M., Simandi, L.I., May, Z., Besenyei, G.,. Coord. Chem. Rev., **2003,** 245, 85.

Maurya, M. R., Sikarwar, S., Joseph, T., Halligudi, S.B., J. Mol Catal A: Chem **2005,** 236, 132.
El-Khalafy, S.H., Hassanein, M., J. Mol Catal A: Chem **2012,** 363, 148.
Hassanein, M., Abdo, M., Gerges, S., El-Khalafy, S.H., J. Mol. Catal. A: Chem. **2008,** 287, 52.
Mukherjee, C., Weyhermuller, T., Bothe, E., Chaudhuri, P., C. R. Chimie **2007,** 10, 313. Bakshi, R., Kumar, R., Mathur, P., Catal Commun. **2012**, 17, 140.
Panja, P., Polyhedron **2012**, 43, 22.
Olmazu, C., Puiu, M., Babaligea, I., Raducan, A., Oancea, D., Appl. Catal. A: General **2012**, 447-448, 74.
Than, R., Feldman, A. A., Krebs, B., Coord. Chem. Rev. **1999,** 182, 211.
Szigyarto, I.C., Simandi, Parkanyi, L.I. Korecz, L. L., Schlosser, G., Inorg. Chem. **2006** 45, 7480.
Blay, G., Fernandez, I., Pedro, J.R., Ruiz, R., Temporal-Sanchez, T., Pardo, E., Loret, F., Munoz, M.C., J. Mol. Catal. A. **2006**, 250, 20;
Majumder, A., Goswami, S., Batten, S.R., Fallah, M.S.E., Ribas, J., Mitra, S., Inorg. Chim. Acta. **2006,** 359, 2375.
Gentschev, P., Moller, N., Krebs, B., Inorg. Chim. Acta **2000,** 300, 442.
May, Z., Simandi, L.I., Vertes, A., J. Mol. Catal. A: **2006,** 266, 239.
Ramadan, A.M., Shaban, S.Y. Ibrahim, M. M., J. Mol. Struct. **2011,** 1006, 348.
Ramadan, A.M., Ibrahim, M.M., El-Mehasseb, I.M., J Coord Chem., **2012,** 65, 13, 2256.
Ramadan, A.M., Shaban, S.Y., van Eldik, R., J. Coord. Chem., **2012,** 65, 14, 20 2415.
Ramadan, A.M., El-Mehasseb, I.M., Issa, R.M., Transition Met. Chem., **2006,** 31, 730
Simandi, T.M., May, Z., Szigyarto, I.C., Simandi, L.I., Dalton Trans. **2005,** 365.
Ramadan, A.M., El-Mehasseb, I.M., Transition Met. Chem., **1998,** 23, 183.
Ramadan, A.M., El-Taras, A.A., EL-Mehasseb I.M., C. R. Chimie, **2012,** 15, 298.
Kaizer, J., Barath, G., Csonka, R., Speier, G., Korecz, L., Rockenbauer, A., Parkanyi, L., J Inorg. Biochem. **2008,** 102, 773.
Kaizer, J., Pap, J., Speier, G.,. Food Chem. **2005,** 93, 425.
Horvath, T., Kaizer, J., Speier, G.,. J. Mol. Catal. A **2004,** 215, 9.
Alcock, N.W., Kingston, R.G., Moore, P., Pierpoint, C., J Chem. Soc., Dalton Trans. **1937,** 1984.
Dornow, A., Menzel, H., Marx, P., Chem. Ber. **1964,** 97, 2173.
Gray, W.J., Coord. Chem. Rev. **1971,** 7, 81.
Coats, A.W., Redfern, J.P., Nature **1964,** 201, 68.
Nakamoto, K., Infrared Spectra of Inorganic and Coordination Compounds, Wiley Interscience, New York **1970**.
Chandra, S., Gupta, L.K., Sangeetika, S., Spectrochim. Acta A **2005,** 62 453.
Silverstein, R.M., Bassler G.C., Morrill, T.C., Spectrometry Identification of Organic Compounds, 4th Ed., Wiley, New York, **1981,** p. 126, 134, 176**.**
Ilham, S., Temel, H., Yilmaz I., Sekerci, M., J. Organometallic. Chem. **2007,** 692, 3855.
Lopaez-Carriga, J.J., Babcock, G.T., Harrison, J.F., J. Am. Chem. Soc. **1986,** 108, 7241.
Rai, P.K., Prased, R. N., Monatsh Chem. **1994,** 125, 385.
Maroney, M. J, Rose, N.J., Inorg Chem. **1984,** 23, 2252.
Nakamoto, K., Infrared and Raman Spectra of Inorganic and Coordination Compounds, Wiley, New York. **1986**
Singh, K., Barwa, M. S., Tyagi, P., Eur J Med Chem. **2007,** 42, 394.
El-Shazly, R. M., El-Hazmi, G.A.A., Ghazy, S.E., El-Shahawi, M.S., El-Shamy, A.A., SpectroChemacta Port, A **2005,** 61, 243.
Kumar, A., Singh, G., Singh, K., Handa, R.N., Dubey, S.N., Proc. Acad. Sci. (India), **2002,** 72A, 11, 87.
Radecka-Paryzek, W., Patroniak-Krzyminiewska, V., Litkowska, H., Polyhedron **1998,** 17, 1477.
Ramadan, A.M., J. Inorg. Biochem., **1997,** 65, 183.
West, D.X., Nassar, A.A., El-Saied, F.A., Ayad, M.I., Transition Met. Chem. **1998**, 23, 321; **1998**, 23, 423.
West, D.X., Huffman, D.L., Saleda, J.S., Liberta, A.E., Transition Met. Chem. **1991,** 16, 565.
West, D.X., Thientaravanich, I., Liberta, A.E., Transition Met. Chem. **1995**, 20, 303.
Lever, A.B.P., Inorganic Electronic Spectroscopy, 2nd ed., Elsevier, New York. **1984**
Onawumi, O.O.E., Faboya, O.O.P., Odunola, O.A., Prasad, T.K., Pajasekharan, M. V., Polyhedron **2008,** 27, 113.
Patel, R. N., Singh, N., Patel, D.K., Gundla, V.L.N., Indian J Chem. **2007**, 422.

El-Metwaly, N.M., Gabr I.M., El-Asmy, A.A., Transition Met. Chem. **2006**, 31, 71.
Selmeczi, K., Reglier, M., Giorgi, M., Speier, G., Coord. Chem. Rev. **2003,** 245 191.
Ismail, K.Z., 1997. Transition Met. Chem., 22, 565; Gang, Z., Yuan, C., Transition Met. Chem., **1994,** 19, 218.
Akbar, A.M., Dey, K.K., Nazimuddin, M., Butcher, R.J., Jasinski, J.P., Jasinski, J.M., Polyhedron **1996,** 15, 331.
Bingham, A.G., Bogge, H., Muller, H., Ainscough, A., Brodie, A.M., J. Chem. Soc. Dalton Trans. **1987**, 493.
El-Shazly, M.F., El-Dissowky, A., Salem, T., Osman, M., Inorg. Chim. Acta **1980**, 40, 1.
Bose, M., Ohta, K., Babu, Y., Sastry, M.D., Chem. Phys. Lett. **2000,** 324, 330.
Ray, R.K., Kauffman, G.B., Inorg. Chim. Acta **1990,** 173, 207.
Hathaway, B.J., Billing, D.E., Coord. Chem. Rev. **1970**, 5, 143.
Sreekanth, A., Krupp, M.R.P., Polyhedron **2003,** 22, 3321.
Hathaway, B.J., Dudley, R.J., Nicholls P., J. Chem. Soc. A **1968**, 1845.
Fidone, I., Stevens, K.W.H., Proc. Phys. Soc. London **1959,** 73,116.
Brown, E.R., Large, R.F., in Techniques of Chemistry: Physical Methods of Chemistry (Eds.: A. Weissberger, B. Rossiter); Wiley: New York, **1971,** Vol. 1, Part IIA, p. 475.
Karlin, K.D., Dahlstrom, P.L., Hyde, I.R., Zubieta, I., J Chem. Soc, Chem. Commun., **1980**, 906.
Makino, N., McMahill, P., Mason, H. S., J. Biol. Chem. **1974,** 249, 6062.
Kupan, A., Kaizer, J., Speier, G., Giorgi, M., Reglier, M., Pollerisz, F., J. Inorg. Biochem. **2009,** 103, 389.
Smith, S.J., Noble, C.J., Palmer, R.C., Hanson, G.R., Schenk, G., Gahan, L. R., Riley, M. J., J. Biol. Inorg. Chem. **2008,** 13, 499.
Voldeba, A., Hol, W.G. J., J. Mol. Biol. **1989,** 209, 249;
Solomon, J.E., Baldwin, M.J., Lowery, M.D., Chem. Rev. **1992,** 92, 521.
Rogic, J.M.M., Swerdloff, M.D., Demmin, T.R., Karlin, K.D., Zubieta, J., Copper Coordination Chemistry: Biochemical and Inorganic Perspectives, Adenine, Guilderland, NY, **1983**.167.
Ramadan, A.M., Issa, R.M., Transition Met. Chem. **2005,** 30, 471.
Karlin, K.D., Gultneh, Y., Nicholson, T., Zubieta, J., Inorg.Chem. **1985,** 24, 3725.
Cox, D., Que, L., J. Am. Chem. Soc. **1988,** 110, 8085.
Malachowski, M.R., Davidson, M. G., Hoffman, J. N., Inorg. Chim. Acta. **1989**, 157, 91. Malachowski, M.R., Davidson, M.G., Inorg. Chim. Acta **1989,** 162, 199.
Malachowski, M.R., Huynh, H.B., Tomlinson, L.J., Kelly, R.S., Furbeejun, J.W., J. Chem. Soc. Dalton Trans **1995,** 31.
Malachowski, M.R., Dorsey, B.T., Parker, M.J., Adams, M.E., Kelly, R.S., Polyhedron **1998,** 17,.8, 1289.
Malachowski, M.R., Dorsey, B., Sackett, J.G., Kelly, R.S., Ferko, A.L., Hardin, R.N., Inorg. Chim. Acta **1996,** 249 85.
Malachowski, M.R., Tomlinson, L.J., Davidson, M.G., Hall, M.J., J. Coord. Chem. **1992,** 25, 171.
Tyson, C.A., Martell, A.E., J. Am. Chem. Soc. **1972,** 94, 939.
Waite, J.H., Anal. Biochem. **1976,** 75, 211.
Golub, E.E., Nishimura, J.S., J. Bacteriol. **1972,** 112, 1353.
Zaki, A.B., El-Sheikh, M.Y., Evans, J., El-Safty, S.A., Polyhedron **2000,** 19, 1317.